2024 Climate-enhanced multispecies stock assessment for walleye pollock, Pacific cod, and arrowtooth flounder in the eastern Bering Sea

Kirstin K. Holsman, Jim Ianelli, Kalei Shotwell, Steve Barbeaux,
Kerim Aydin, Grant Adams, Kelly Kearney, Anna Sulc, Sophia Wassermann

Contents

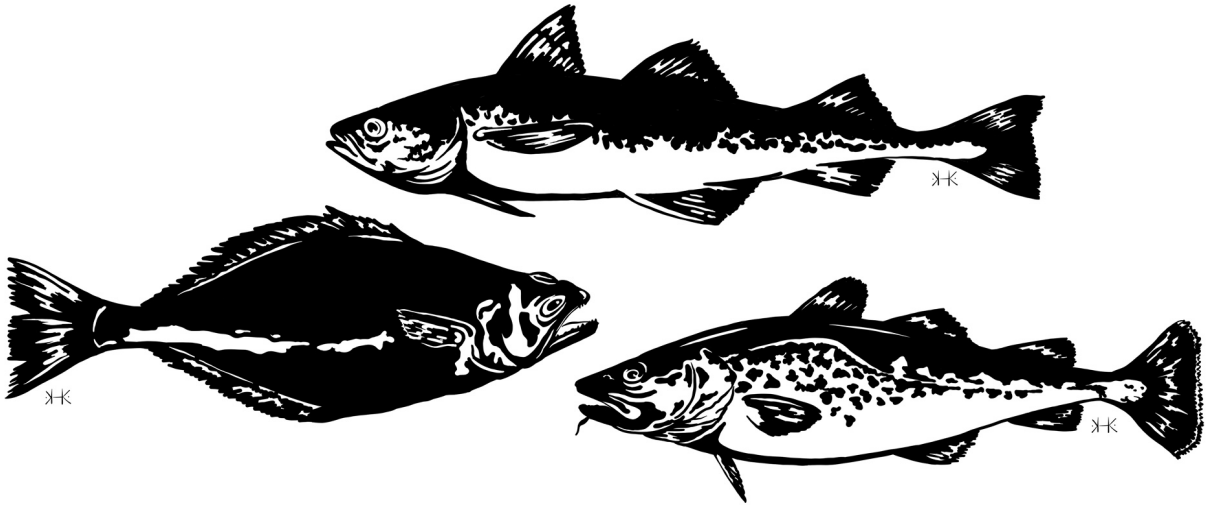

November 2024 | kirstin.holsman@noaa.gov Alaska Fisheries Science Center, National Marine Fisheries Service, NOAA, 7600 Sand Point Way N.E., Seattle, Washington 98115

Suggested citation: *Holsman, K. K., J. Ianelli, K. Shotwell, S. Barbeaux, K. Aydin, G. Adams, K. Kearney, A. Sulc, S Wassermann (2024) Climate-enhanced multispecies stock assessment for walleye pollock, Pacific cod, and arrowtooth flounder in the eastern Bering Sea. North Pacific Fishery Management Council, Anchorage, AK.*

1 Overview

This is a three species stock assessment for walleye pollock (*Gadus chalcogrammus*), Pacific cod (*Gadus macrocephalus*) and arrowtooth flounder (*Atheresthes stomias*), from the Eastern Bering Sea (EBS), Alaska updated from Holsman et al.(2016) and incorporating climate informed reference points as detailed in Holsman et al. (2020a,b). Results are presented from models estimated and projected without trophic interactions (single-species mode, SSM) and with trophic interactions (multispecies mode, MSM). The main features and settings for this multispecies model include:

- Survey biomass and harvest indices from the NEBS and SEBS are included.
- Predation natural mortality is age specific and annually varying (M2). Residual (non-predation) natural mortality (M1) is age specific but not-annually varying and differs slightly from current assessments for each species (see Table 3 below).
- The multispecies mode uses the the residual mortality vectors of current single species assessment models for pollock, Pacific cod, and arrowtooth flounder except for the ages 1 and 2 mortality rates for pollock, which were adjusted downward to 0.01 and 0.30, respectively.
- Pollock fishery composition data is age-based where as Pacific cod and arrowtooth fishery composition data is based on lengths.
- Predator overlap index is set to 1 for all species (i.e., all prey are available to all predators).
- Weights at age for pollock are based on values from the 2024 SAFE report; for Pacific cod and arrowtooth, they are calculated outside of the model using a temperature-dependent von Bertalanffy to fill in for missing years between 1979-2012 and assume 2012 weight at ages for 2013-2024. For projections, all three species use temperature-specific weights at age using the temperature-dependent von Bertalanffy for 1979-2012.
- Acoustic trawl survey selectivity was set equal to the SAFE report model estimates. Fisheries selectivity and survey selectivity are age specific and constant over time.
- Predator-prey suitability is age-specific and constant over time.
- Arrowtooth flounder stock is treated as sexes combined (weight at age and proportion mature is calculated separately for males and females and combined using a mortality-based mean).
- Maturity schedules are based on 2012 assessments and differ slightly from SAFE assessments.
- Projections to derive ABC include a sequential method for determining universal climate-naive B0, and include the constraint that $\text{SSB}_F > 0.35\text{SSB}_0$ for all years in the projection.
- A moderately "climate-informed" approach is used to derive biological reference points through projecting the model forward with climate effects on weight at age and predation mortality but with a climate-naive Ricker stock recruitment curve (i.e., without environmental covariates).
- Evaluation of spawning stock biomass given F_{ABC} for 2025 and 2026 and is performed using an ensemble of warming scenarios.
- Evaluation of spawning stock biomass given F_{ABC} for 2034, 2050, and 2080 under low, medium, and high warming scnearios is performed using an ensemble of warming scenarios from the Alaska Climate Integrated Modeling project (ACLIM).

1.1 Key 2024 updates

- Survey biomass and harvest from the NEBS and SEBS were updated through 2024.
- Survey biomass and age or length composition were updated using data available from the NMFS bottom trawl survey and fishery observer database 2024.
- Bottom temperature and other variables from the 2024 BERING10K operational hindcast using the 30 layer model (K20) was updated through 2024.
- Residual natural mortality (M1_{ij}) for ages 1-4 of all three species was set to the mean of the total natural mortality from the multispecies assessment for years 1979 - 2024. Natural mortality for older Pacific cod was set to 0.38 for to match the Pacific cod stock assessment (Thompson et al. 2018).
- The newest set of ACLIM high resolution climate projections for the Bering sea (Hermann et al, 2021, Cheng et al. 2021) were used to drive projections and derive F_{target} and ABC under climate effects. This

includes a broader suite of scenarios from High carbon mitigation (ssp126) to low carbon mitigation scenarios (ssp585).
- Climate effects on recruitment were included in the projection model suite for 2024, sensu Holsman et al. 2020.
- More detailed information was included for temperature specific weight at age and climate-driven recruitment.
- Estimated of annual biomass of key prey species eaten (NEBS and SEBS combined) were produced for species outside of the assessment (e.g., *"Opilio"*) based on model estimates of ration (kg eaten/pred) and abundance.

1.2 Response to Council, SSC or Plan Team comments

- Plan Team recommendations from Nov. 2023 included 'the author intends to communicate with stock assessment authors earlier in next year's assessment cycle to help facilitate risk assessment, which is further recommended by the Team".

1.3 SSC Recommendations from Dec 2023 relating to the multi-species model:

- The SSC agrees with the BSAI GPT's proposal in their presentation to move the multi-species model out of the pollock stock assessment, where it has been included as an appendix since it was first developed. Instead, they suggested it would be a separate chapter listed in parallel with the ESR, as it applies to multiple stocks and informs the ESRs.
- The SSC recognizes the multi-species model as a 'research model' and therefore recommends placing information that appears comparable to a stock assessment specifications table in a regular table (at the end of the document) in order to avoid confusion.
- The SSC supports the multi-species model authors' plan to work with individual assessment authors early in the process to facilitate incorporation of those results into stock assessments.
- Weight-at-age in the multi-species model is temperature driven based on a bioenergetic model. It would be useful to compare these estimates to empirical weights-at-age or the random effects model estimates of weight-at-age in the main pollock assessment.
- Consider how output from the multispecies model may best be interpreted independently from results of the actual stock assessment without drawing inference from the same data twice.

---

2 Introduction

2.1 Multispecies modeling

Multispecies statistical catch-at-age models (MSCAA) are an example of a class of Models with Intermediate Complexity for Ecosystem assessments (i.e., MICE; Plaganyi et al., 2014), which have particular utility in addressing both strategic and tactical EBFM questions (Hollowed et al. 2013; Fogarty 2014; Link and Browman 2014; Plaganyi et al., 2014, Holsman et al. 2020, Adams et al. 2022). MSCAA models may increase forecast accuracy, may be used to evaluate propagating effects of observation and process error on biomass estimates (e.g., Curti 2013; Ianelli et al., 2016), and can quantify climate and trophic interactions

on species productivity. As such MSCAA models can address long recognized limitations of prevailing single species management, notably non-stationarity in mortality and biological reference points, and may help reduce risk of over-harvest, especially under climate change (Link 2010; Plaganyi et al., 2014; Fogarty 2014). Multispecies biological reference points (MBRPs) from MSCAA model are conditioned on the abundance of other species in the model (Collie and Gislason 2001; Plaganyi et al., 2014; Fogarty 2014), thus they may also have utility in setting harvest limits for multispecies fleets, evaluating population dynamics in marine reserves or non-fishing areas, and quantifying trade-offs that emerge among fisheries that impact multiple species in a food web (see reviews in Pikitch et al., 2004; Link 2010; Levin et al., 2013; Link and Browman 2014; Fogarty 2014).

Depending on their structure, MSCAA models can be used to evaluate climate- and fisheries-driven changes to trophodynamic processes, recruitment, and species abundance (Plaganyi et al., 2014). MSCAA models differ somewhat among systems and species, but most use abundance and diet data to estimate fishing mortality, recruitment, stock size, and predation mortality simultaneously for multiple species in a statistical framework. Similar to age structured single species stock assessment models widely used to set harvest limits, MSCAA models are based on a population dynamics model, the parameters of which are estimated using survey and fishery data and maximum likelihood methods (e.g., Jurado-Molina et al., 2005; Kinzey and Punt, 2009; Van Kirk et al., 2010; Kempf 2010; Curti et al., 2013; Tsehaye et al., 2014). Unlike most single-species models (but see Hollowed et al. 2000b; Spencer et al. 2016), MSCAA models additionally separate natural mortality into residual and annually varying predation mortality, and model the latter as a series of predator-prey functional responses. Thus, natural mortality rates for each species in MSCAA models depend on the abundance of predators in a given year and vary annually with changes in recruitment and harvest of each species in the model.

MSCAA models have specific utility in quantifying direct and indirect effects of fisheries harvest on species abundance and size distributions (see reviews in Hollowed et al., 2000a, 2013; Link 2010; Fogarty 2014; Link and Browman 2014; Plaganyi et al., 2014), which is important for EBFM and trade-off analyses of various management strategies under climate change. Rapidly shifting climate conditions are also of growing concern in fisheries management as changes in physical processes are known to influence individual growth, survival, and reproductive success of fish and shellfish (Hanson et al., 1997; Kitchell et al., 1977; Morita et al., 2010; Hollowed et al., 2013, Cheung et al., 2015, Holsman et al. 2020). Climate-driven changes in water temperature can directly impact metabolic costs, prey consumption, and somatic or gonadal tissue growth, with attendant indirect effects on survival, production, and sustainable harvest rates (e.g., Hanson et al., 1997; Morita et al., 2010, Cheung et al., 2015, Holsman and Aydin, 2015). Temperature-dependent predation, foraging, metabolic, and growth rates are common in more complex spatially-explicit food web or whole of ecosystem models such as GADGET (e.g., Howell and Bogstad 2010; Taylor et al., 2007), Atlantis (e.g., Fulton et al., 2011; Kaplan et al., 2012; 2013), and FEAST (Ortiz et al., 2016). Temperature functions for growth and predation can also be incorporated into MSCAA models, allowing this class of models to be used to evaluate interacting climate, trophodynamic, and fishery influences on recommended fishing mortality rates.

Numerous studies point to the importance of using multispecies models for EBFM (see review in Link 2010). Multispecies production models produced different estimates of abundances and harvest rates than single species models for Northeast US marine ecosystems (Gamble and Link, 2009; Tyrrell et al., 2011), and MSY of commercial groundfish stocks estimated from aggregated production models were different than the sum of MSY estimates from single-species assessments (Mueter and Megrey, 2006; Gaichas et al., 2012; Smith et al., 2015). Multispecies models have been used to demonstrate long-term increases in yield of Icelandic stocks of Atlantic cod (*Gadus morhua*) and reductions in capelin (*Mallotus villosus*) and Northern shrimp (*Pandalus borealis*) catch associated with short-term decreases in cod harvest (Danielsson et al., 1997). Kaplan et al. (2013) demonstrated the disproportionately large ecosystem impacts of applying the same Fx% harvest control rule approach to forage fish as is used for groundfish in the northeast Pacific, and separately, accounting for trophodynamics in a southern Benguela ecosystem resulted in higher carrying capacity for small pelagic species under fishing (versus no-fishing) scenarios (Smith et al., 2015).

Since natural mortality and recruitment rates in a MSCAA model are conditioned on harvest rates of predators in the model, an ongoing area of research is evaluating MSCAA model analogs to single-species

biological reference points (see Moffitt et al., 2016), such as harvest rates that correspond to maximum yield (FMSY) or proxies thereof (e.g., Fx%). Other multispecies models have been used to derive and evaluate MBRPs, although these have largely focused on MSY (e.g., Kaplan et al., 2013; Smith et al., 2015). A notable exception is Collie and Gislason (2001), who evaluated a variety of MBRPs using a multispecies, virtual population analysis and found MBRPs to be sensitive to variation in natural mortality (much less so to variability in growth), and as such proposed that fishing mortality reference levels for prey species with high mortality be conditioned on the level of predation mortality. Building on this approach, Moffitt et al. (2016) demonstrated a projection approach for using multispecies models to derive a variety of MBRPs for EBFM. This provides a basis for the application of MSCAA models for increased use in tactical and strategic EBFM decision-making across a diversity of management frameworks worldwide.

2.2 CEATTLE model

Here we present results from a three species climate-enhanced MSCAA model for the Bering Sea (hereafter CEATTLE, for Climate-Enhanced, Age-based model with Temperature-specific Trophic Linkages and Energetics) that includes temperature-dependent von Bertalanffy weight-at-age functions (VBGF; von Bertalanffy, 1938) and temperature-specific, bioenergetics-based predation interactions. The eastern Bering Sea (Alaska), is defined by large, climate-driven changes to trophodynamics and species productivity that can vary on annual and multi-annual timescales (see reviews in Aydin and Mueter 2007; Hunt et al., 2011; Stabeno et al., 2012; Baker et al., 2014). Accordingly, fisheries management in Alaska has a long history of using ecosystem information and multispecies models for strategic management advice (e.g., multispecies model-based indices, such as mean trophic level, are regularly reported in the annual Ecosystem Considerations chapter of Alaska Stock Assessment and Fishery Evaluation (SAFE) reports; see review in Livingston et al., 2011). Development of multiple MSCAA models in the region (Jurado-Molina et al., 2005; Kinzey and Punt , 2009; Van Kirk, 2010, Holsman et al. 2016, Adams et al. 2022) has advanced regional EBFM, facilitating use of estimates from MSCAA models in tactical single-species management advice. For instance, the CEATTLE multispecies model had been included as an appendix to the BSAI pollock assessment (Ianelli et al. 2019) from 2016 - 2023, and has been used annually since 2016 to product Ecosystems Status Report and Ecosystem and SocialEconomic Profile indices for the Bering Sea, and in 2024 the assessment is now a stand alone chapter. Similarly, Dorn et al. (2014) recently evaluated predation mortality estimates from a regional MSCAA model developed by Van Kirk (2010) to inform natural mortality for the Gulf of Alaska walleye pollock (*Gadus chalcogrammus*, hereafter pollock) stock assessment and Adams et al. (2022) extended the CEATTLE modeling framework to the GOA to evaluate climate and harvest scenarios in that system and produce indices for the GOA Ecosystem Status Report.

Climate-enhanced MSCAA like CEATTLE, have considerable utility in accounting for climate effects on harvest and are useful for species that exhibit strong trophic interactions (predator and prey species) or contrasting management or biological constraints that require simultaneous evaluation (Link 2010). In the eastern Bering Sea, pollock are both predators (adults) and prey for a variety of species including cannibalistic conspecifics (e.g., Boldt et al., 2012; Dunn and Matarese, 1987; Nishiyama et al., 1986). Variable climate conditions, particularly the spatial extent of winter sea ice, the timing of sea ice spring melt, and subsequent summer bottom temperatures, can differentially promote survival of pollock and their predators and/or modulate predator and prey overlap in the region (e.g., Baily 1989; Zador et al., 2011; Boldt et. al 2012; Hunsicker et al. 2013; Baker and Hollowed 2014). Diet analyses suggest Pacific cod (*Gadus macrocephalus*), cannibalistic conspecifics, and arrowtooth flounder (*Atheresthes stomias*), among others, are important predators of pollock populations in the eastern Bering Sea (Livingston 1993; Aydin and Mueter 2007; Mueter et al., 2007). Climate driven changes to food webs, thermal experience, distribution, and growth collectively impact natural mortality for juveniles, especially juvenile pollock. Accounting for these multispecies interactions is increasingly important under climate-driven change (Holsman et al. 2019,2020, Karp et al. 2019).

3 Methods

3.1 Multispecies population dynamics

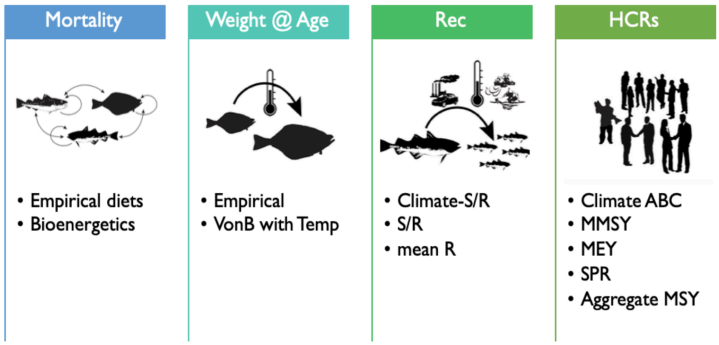

Figure 1: CEATTLE (Bering Sea version) optional features.

The CEATTLE model is an environmentally-enhanced stock assessment model (sensu Link 2010), where temperature-specific algorithms predict size-at-age and predation mortality. CEATTLE is programmed in AD model builder (Fournier et al., 2012), and builds on earlier models that combine catch-at-age assessment models with multispecies virtual population analysis (MSVPA) in a statistical framework (i.e., Jurado-Molina et al., 2005). Abundance and biomass of each cohort is modeled using standard population dynamics equations, accounting for a plus age group (Table 1, Eqs. (1), (2)). The initial age-structure is assumed to correspond to unfished equilibrium, and the numbers of each species i at age j in year 1 ($N_{0,ij}$) are treated as estimable parameters (Eq. (1)), such that:

$$N_{ij,1} = \begin{array}{lll} R_{0,i}e^{(-j\ \mathrm{M1}_{ij})}N_{0,ij} & y = 1 & 1 < j < A_i \\ R_{0,i}e^{(-j\ \mathrm{M1}_{i,A_i})}N_{0,i,A_i}/\left(1 - e^{(-\mathrm{M1}_{i,A_i})}\right) & y = 1 & j \geq A_i \end{array} \tag{1}$$

The number of each species i, age a each year y is then:

$$\begin{array}{lll} N_{i,j+1,y+1} = N_{i,j,y}e^{-Z_{ij,y}} & 1 \leq y \leq n_y & 1 \leq j < A_i - 1 \\ N_{i,A_i,y+1} = N_{i,A_i-1,y}e^{-Z_{i,A_i-1,y}} + N_{i,A_i,y}e^{-Z_{i,A_i,y}} & 1 \leq y \leq n_y & j \geq A_i \end{array} \tag{2}$$

Total mortality of each prey species i, age j (or predator species p age a) in each year y is the sum of mortality due to predators in the model ($\mathrm{M2}_{ij,y}$), fishing mortality ($\mathrm{F}_{ij,y}$), and residual mortality ($\mathrm{M1}_{ij}$), Eq. T1.6). Predation mortality (Eq. T2.1) is based on the assumption that the annual age-specific ration of a predator is allocated to prey species of a given age according to predator selectivity (Table 2, Eq. T.2.2). Predator selectivity is based on the suitability function derived by Jurado-Molina et al. (2005) and fit to available data from 1981-2015, while annual ration is a function of temperature-specific allometric relationships between ration and fish weight based on bioenergetics models for each species (Eqs. T2.4 and T2.5; see Holsman et al. 2016, and Holsman and Aydin, 2015 for more detail).

The length-to-weight relationships, predator size and species diet preference, bioenergetics-based, temperature-specific predator rations, and maturity were based on previous studies (Tables 1 and 2; Table 5; Holsman et al. Holsman and Aydin, 2015, Holsman et al. 2016). Size-specific diet compositions for each species were assumed known based on diet data collected during the AFSC bottom trawl survey (i.e., diet data were not included in the objective function) and trophic patterns in survey and fishery-based diet data were used to calculate mean (across years and stations) predator-prey suitability (Eq. T2.2).

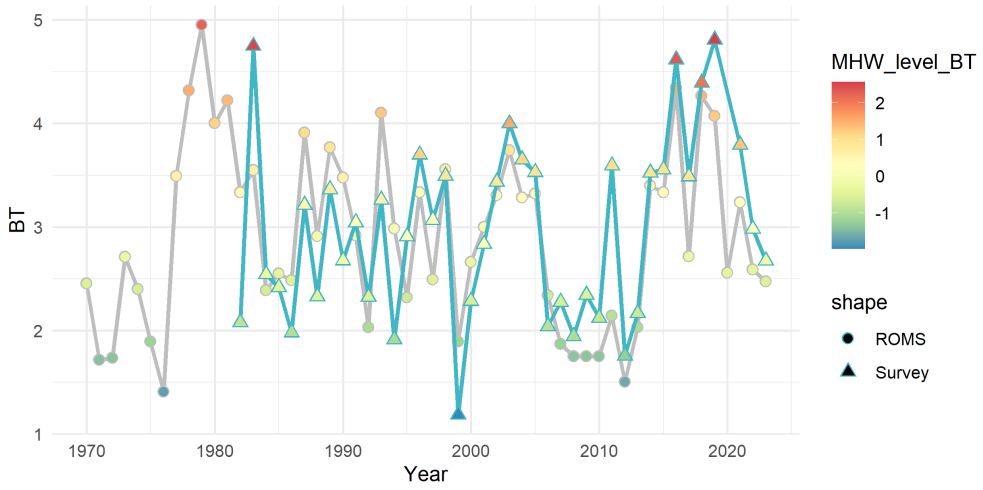

Figure 2: Mean summer bottom temperature (BT, in deg. C) for the eastern Bering Sea as observed on NMFS summer ground fish survey in the EBS (triangles). Circles represent the opertational Bering10K 30 layer high resolution oceanpgraphic model hindcast for bottom tempteratures used in this assessment (Kearney et al. 2020).

3.2 Temperature specific weight at age

Water temperature is known to directly impact growth through influencing metabolic and digestion rates, which often scale exponentially with body weight and temperature (see Hanson et al., 1997 for an overview). Thus we modified the generalized formulation of the von Bertalanffy growth function (VBGF; von Bertalanffy 1938; Pauly 1981; Temming 1994) to predict temperature-dependent growth by allowing the allometric scaling parameter d to increase with temperature (Eq. (2)). Essington et al. (2010) and Holsman and Aydin (2015), and Holsman et al. (2016) describe the derivation and application of the VBGF towards bioenergetics modeling in great detail, so we do not repeat it here. Essentially, in this formulation d represents the realized allometric slope of consumption, which integrates both the direct effect of temperature on consumption and indirect ecological interactions that scale with temperature and influence relative foraging rates (see Essington et al., 2010; Holsman and Aydin, 2015). We fit the VBGF to otolith-based length- and weight-at-age data (n = 21,388, 14,362, and 772, for pollock, Pacific cod, and arrowtooth flounder, respectively) collected during AFSC Bering Sea surveys and analyzed at the AFSC such that:

$$W_{ij,y} = W_{\infty,iy}(1 - e^{(-K_i(1-d_{i,y})(j-t_{0,i}))})^{1/(1-d_{i,y})}e^{\varepsilon}, where \varepsilon\ N(0, \sigma^2_{d,i}) \tag{3}$$

where $t_{0,i}$ is the age at which $W_{ij,y} = 0$, $W_{\infty,iy}$ is the asymptotic mass which can vary by species i and year y (i.e., $W_{\infty,iy} = (H_i/K_i)^{1(1-d_{i,y})}$), H_i is the assimilation constant K_i is the energy loss constant (Essington et al., 2010), and ε is a normally and independently distributed random variable with mean 0 and variance $\sigma^2_{d,i}$. Essington et al. (2010) and Holsman and Aydin, (2015) statistically estimated the d, K and H parameters for various species to estimate consumption rates. In particular, Holsman and Aydin (2015) found that the d parameter varied between species and regions in Alaska (USA). We further modified this approach to estimate d annually for each year y in the dataset, as a linear function of temperature T_y such that:

$$d_{i,y} = e^{(\alpha_{d,i,y} + \alpha 0_{d,i} + \beta_{d,i}T_y)} \tag{4}$$

where $\alpha 0_{d,i}$ and $\alpha_{d,i,y}$ represent the mean d intercept and $\beta_{d,i}$ is the coefficient for the residual effect of temperature on the d consumption parameter (see https://github.com/NOAA-REEM/vonBEE for code and examples (under development until after publication of the revised analysis in 2024). We chose this formulation based on the empirical relationship between temperature and consumption, assuming that d

would capture the differential effects of temperature on growth, and that waste rates scale proportionally with weight but do not vary over time with diet or temperature (i.e. K is constant but d can vary with temperature). This formulation allows both the slope and asymptotic limit of growth to vary with temperature (Fig. 3). Similar approaches, with slightly different modifications to the VBGF, including temperature and prey specific terms for d and K, respectively, have been used elsewhere to evaluate climate impacts on fish growth (e.g., Cheung et al., 2015; Hamre, 2003).

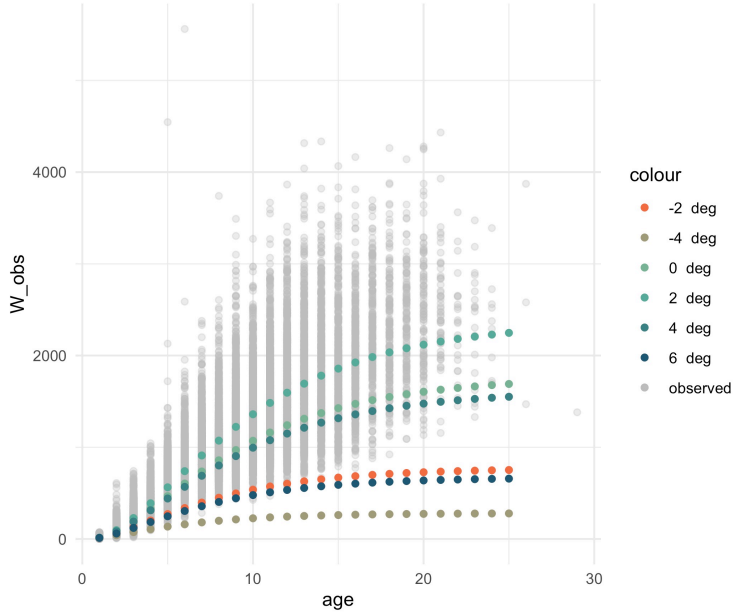

Figure 3: Example fit of the VonB with Temperature model (here for EBS pollock where bottom temperature (Temp) and Temp2 are predictor variables.

Table 1. Population dynamics equations for species i and age j in each simulation year y. BT indicates the AFSC bottom trawl survey and EIT represents the echo-integrated acoustic-trawl survey. For all other parameter definitions see Table 3.

Definition	Equation		
Recruitment	$N_{i,1,y} = R_{i,y} = R_{0,i}e^{\tau_{i,y}}$	$\tau_{i,y} \sim N(0, \sigma^2)$	T1.1
Catch (numbers)	$C_{ij,y} = \frac{F_{ij,y}}{Z_{ij,y}}\left(1 - e^{-Z_{ij,y}}\right) N_{ij,y}$		T1.2
Total yield (kg)	$Y_{i,y} = \sum_j^{A_i}\left(\frac{F_{ij,y}}{Z_{ij,y}}\left(1 - e^{-Z_{ij,y}}\right) N_{ij,y} W_{ij,y}\right)$		T1.3
Biomass at age (kg)	$B_{ij,y} = N_{ij,y} W_{ij,y}$		T1.4
Spawning biomass at age (kg)	$SSB_{ij,y} = B_{ij,y}\rho_{ij}$		T1.5
Total mortality at age	$Z_{ij,y} = \mathrm{M1}_{ij} + \mathrm{M2}_{ij} + F_{ij}$		T1.6
Total mortality at age	$F_{ij,y} = F_{0,i}e^{\epsilon_{i,y} S^f_{ij}}$	$\epsilon_{i,y} \sim N\left(0, \sigma^2_{\mathrm{F},i}\right)$	T1.7
Weight at age (kg)	$W_{ij,y} = W_{\infty,iy}\left(1 - e^{\left(-K_i(1-d_{i,y})(j-t_{0,i})\right)}\right)^{\frac{1}{1-d_{i,y}}}$		T1.8a
	$d_{i,y} = e^{\left(\alpha_{d,i,y} + \alpha_{0,d,i} + \beta_{d,i}T_y\right)}$		T1.8b
	$W_{\infty,iy} = \left(\frac{H_i}{K_i}\right)^{1/(1-d_{i,y})}$		T1.8c
Bottom trawl survey biomass (kg)	$\hat{\beta}^s_{i,y} = \sum_j^{A_i}\left(N_{ij,y}e^{-0.5Z_{ij,y}} W_{ij,y} S^{\mathrm{S}}_{ij}\right)$		T1.9
Acoustic survey biomass (kg)	$\hat{\beta}^{eit}_{y} = \sum_j^{A_i}\left(N_{1j,y}e^{-0.5Z_{1j,y}} W_{1j,y} S^{eit}_{1j} q^{eit}_{1,j}\right)$	(pollock only)	T1.10

Definition	Equation		
Fishery age composition	$\hat{O}^f_{ij,y} = \frac{C_{ij,y}}{\sum_j C_{ij,y}}$		T1.11
Bottom trawl age composition	$\hat{O}^s_{ij,y} = \frac{N_{ij,y} e^{0.5(-Z_{ij,y})S^{\mathrm{S}}_{ij}}}{\sum_j \left(N_{ij,y} e^{0.5(-Z_{ij,y})S^{\mathrm{S}}_{ij}}\right)}$		T1.12
Acoustic trawl age composition	$\hat{O}^{eit}_{1j,y} = \frac{N_{1j,y} e^{-0.5 Z_{1j,y}} S^{eit}_{1j} q^{eit}_{1,j}}{\sum_j \left(N_{1j,y} e^{-0.5 Z_{1j,y}} S^{eit}_{1j} q^{eit}_{1,j}\right)}$	(pollock only)	T1.13
Bottom trawl selectivity	$S^{\mathrm{s}}_{ij} = \frac{1}{1+e^{\left(-b^{\mathrm{S}}_i \cdot j - a^{\mathrm{S}}_i\right)}}$		T1.14
Fishery selectivity	$S^f_{ij} = e^{\eta_{ij}} \quad j \le A_{\eta,i}$ $S^f_{ij} = e^{\eta_{ij}} A_{\eta,i} \quad j > A_{\eta,i}$	$\eta_{ij} \sim N\left(0, \sigma^2_{f,i}\right)$	T1.15
Proportion female	$\omega_{ij} = \frac{e^{-jM_{\mathrm{fem}}}}{e^{-jM_{\mathrm{fem}}} + e^{-jM_{\mathrm{male}}}}$		T1.16
Proportion of mature females	$\rho_{ij} = \omega_{ij}\phi_{ij}$		T1.17
Adjusted weight at age (kg)	$W_{ij,y} = W^{\mathrm{fem}}_{ij,y}\omega_{ij} + (1-\omega_{ij})W^{\mathrm{male}}_{ij,y}$		T1.18
Adjusted residual natural mortality (kg)	$\mathrm{M1}_{ij} = \mathrm{M1}^{\mathrm{fem}}_{ij}\omega_{ij} + (1-\omega_{ij})\mathrm{M1}^{\mathrm{male}}_{ij,y}$		T1.19

We used this approach to derive annual temperature-specific coefficients of d for pollock and Pacific cod (combined sexes) and separately for male and female arrowtooth flounder (Table 3; Table 6). For arrowtooth flounder, we then used the age-specific proportions of mature females (ρ_{ij}) and males ($1-\rho_{ij}$) to derive the mean weight-at-age for both sexes combined (Eq. T1.18 and Table 5). Lastly, male and female natural mortality rates (M_{male} and M_{fem} , respectively) and age-specific maturity proportions (ϕ_{ij}) from the 2012 stock assessments for eastern Bering Sea pollock (Ianelli et al., 2012), and Bering Sea and Aleutian Islands Pacific cod (Thompson and Lauth, 2012) and arrowtooth flounder (Spies et al., 2012), were used to derive estimates of the proportion of mature females at age (ρ_{ij}; Eq. T1.17).

Table 2. Predation mortality ($M2$) equations for predators p of age a, and prey i of age j.

Definition	Equation	
Predation mortality	$\mathrm{M2}_{ij,y} = \sum_{pa}\left(\frac{N_{pa,y}\delta_{pa,y}\bar{S}_{paij}}{\left(\sum_{ij}\bar{S}_{paij}B_{ij,y}\right)+B^{other}_p\left(1-\sum_{ij}\left(\bar{S}_{paij}\right)\right)}\right)$	T2.1
Predator-prey suitability	$\bar{S}_{paij} = \frac{1}{n_y}\sum_y\left(\frac{\frac{\bar{U}_{paij}}{\theta_{pi,y}B_{ij,y}}}{\sum_{ij}\left(\frac{\bar{U}_{paij}}{\theta_{pi,y}B_{ij,y}}\right)+\frac{1-\sum_{ij}\bar{U}_{paij}}{\theta_{other,y}B^{other}_p}}\right)$	T2.2
Mean gravimetric diet proportion	$\bar{U}_{paij} = \sum_y \frac{U_{paijy}}{n_y}$	T2.3
Individual specific ration (kg yr^{-1})	$\delta_{pa,y} = \hat{\varphi}_{pa,y}\alpha_\delta W^{(1+\beta_\delta)}_{pa,y} f\left(T_y\right)_p$	T2.3
Temperature scaling consumption algorithm	$f\left(T_y\right)_p = V^X e^{(X(1-V))}$	T2.5
	$V = \left(T^{cm}_p - T_y\right) / \left(T^{cm}_p - T^{co}_p\right)$	T2.5a
	$X = \left(Z^2\left(1+\left(1+40/Y\right)^{0.5}\right)^2\right)/400$	T2.5b
	$Z = ln\left(Q^c_p\right)\left(T^{cm}_p - T^{co}_p\right)$	T2.5c
	$Y = ln\left(Q^c_p\right)\left(T^{cm}_p - T^{co}_p + 2\right)$	T2.5d

3.3 Parameter estimation & data

The parameters of the model are either pre-specified or estimated by selecting parameters that minimize the log-likelihood function (Table 3) and include fishing mortality rates ($F_{ij,y}$), fishery and survey selectivity (s^{f}_{ij} and s^{s}_{ij} , respectively), initial (pre-harvest) abundance in year 1979 ($N_{0,ij}$), and annual recruitment ($R_{i,y}$), while the estimable parameter of the likelihood function is the catchability coefficient for the acoustic survey (q_1^{eit}; Table 3; Table 4). We used summer bottom temperature indices from the Bering10K ROMSNPZ model (Fig. 2) to drive weight at age and bioenergetics sub-models. We fit the model to available survey and fishery data for the eastern Bering Sea including biomass estimates and age-composition data from the annual AFSC summer bottom trawl survey for the NEBS and SEBS sub-regions combined (Table 5; Fig. 4), biomass and age-composition data from the AFSC Acoustic-trawl (AT) survey (pollock only), and the total fishery catch and fishery age-composition data collected by AFSC observers and analyzed at AFSC (NEBS and SEBS) (Hilborn and Walters, 1992; Quinn and Deriso, 1999). Penalties were imposed on the changes over age in fishery selectivity. Likelihood priors were applied to normalize the log of annual recruitment and the fisheries mortality deviations, as well as initial abundances (Table 5). Selectivity for the AT survey was set to previously reported values (Table 3; Honkalehto et al., 2011; Ianelli et al., 2012).

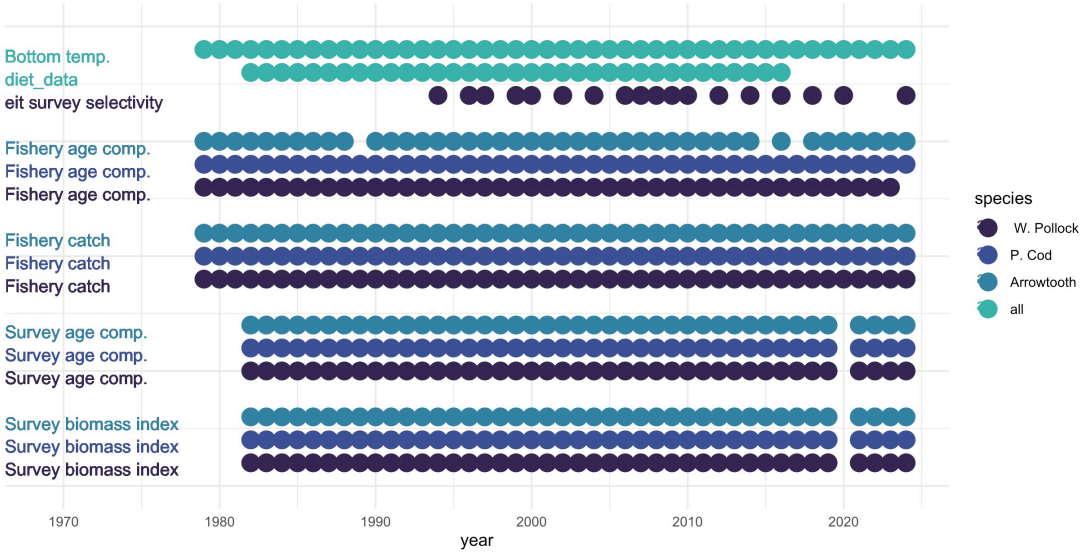

Figure 4: Data and years used for each species

Table 3. Parameter definition (n) is the number of parameters for estimated parameters only, value, data source, and type: (I) Input parameter (assigned); (M) model index; (E) Estimated parameter; (F) fixed parameter; (P) Derived quantity;(D) Data.

Parameter	Definition	Type	Value	Source
y	Year	M	$[1, 2, 3 \dots n_y]$	e
p	Predator	M	$[1, 2, 3 \dots n_p]$	e
a	Predator age (years)	M	$[1, 2, 3 \dots A_p]$	e
i	Prey	M	$[1, 2, 3 \dots n_i]$	e
j	Prey age (years)	M	$[1, 2, 3 \dots A_i]$	e
n_i	Number of prey species	I	3	e
n_p	Number of predator species	I	3	e
$R_{0,i}$	Mean Recruitment; $n = [1, 1, 1]$	E	≥ 0	e
$\tau_{i,y}$	Annual recruitment deviation; $n = [34, 34, 34]$	E	number	e
$N_{0,ij}$	Initial abundance; $n = [11, 11, 20]$	E	≥ 0	e

Parameter	Definition	Type	Value	Source
$F_{0,i}$	Mean fishing mortality; $n = [1, 1, 1]$	E	≥ 0	e
$varepsilon_{i,y}$	Annual fishing mort. deviation; $n = [34, 11, 20]$	E	number	e
η_{ij}	Fishery age selectivity coef. ; $n = [8, 8, 8]$	E	number	e
b_i^{s}	Survey age selectivity slope; $n = [1, 1, 1]$	E	number	e
a_i^{s}	Survey age selectivity limit ; $n = [1, 1, 1]$	E	number	e
$d_{i,y}$	VBGF allometric slope of consumption	P	≥ 0	e
$W_{\mathrm{inf},iy}$	VBGF max asymptotic weight (kg)	P	> 0	e
ρ_{ij}	Proportion of mature females at age	P	$\in [0, 1]$	e
$\mathrm{M1}_{ij}$	Residual natural mortality	F	≥ 0	e, h
n_y	Number of estimation years	I	46	e
y_0	Start year	I	1979	e
ω_{ij}	Female proportion of population	F	$\in [0, 1]$	c
ϕ_{ij}	Age-specific maturity proportions	F	$\in [0, 1]$	c
$C_{i,y}^{*}$	Observed total yield (kg)	D	≥ 0	f
$O_{ij,y}^{\mathrm{f}}$	Observed fishery age comp.	D	$\in [0, 1]$	f
$O_{ij,y}^{\mathrm{s}}$	Observed BT age comp.	D	$\in [0, 1]$	b
$O_{1j,y}^{\mathrm{eit}}$	Observed AT age comp.	D	$\in [0, 1]$	g
$\beta_{i,y}^{\mathrm{s}}$	Observed BT survey biomass (kg)	D	number	b
β_y^{eit}	Observed AT survey biomass (kg)	D	number	g
T_y	Bottom temperature (^oC)	D	number	b
$U_{paij,y}$	Gravimetric proportion of prey in predator stomach	D	$\in [0, 1]$	b
B_p^{other}	Biomass of other prey (kg)	D	$0 \geq$	h
S_{1j}^{eit}	AT survey selectivity	F	$\in [0, 1]$	c

Table 3 (continued). Parameter, definition, species-specific value (Pollock; (Cod) Pacific cod; (ATF) Arrowtooth flounder both sexes; (M:) Arrowtooth flounder males; (F:) Arrowtooth flounder females), and type: (I) Input parameter (assigned); (M) model index; (E) Estimated parameter; (F) fixed parameter; (P) Derived quantity;(D) Data.

Parameter	Definition	Type	Pollock	Cod	ATF	Source
A_i	Number of prey ages	I	12	12	21	e
A_p	Number of predator ages	I	12	12	21	e
$\hat{\varphi}_p$	Annual relative foraging rate (d yr^{-1})	I				d
α_δ	Intercept of the allometric maximum consumption function (g g^{-1} yr^{-1})	I	0.119	0.041	0.125	a
β_δ	Allometric slope of maximum consumption	I	-0.460	-0.122	-0.245	a
T_p^{cm}	Consumption maximum physiological temperature (^{o}C)	I	15.00	21.00	34.13	a
T_p^{co}	Consumption optimum physiological temperature (^{o}C)	I	10.00	13.70	19.60	a
Q_p^c	Max consumption parameter	I	2.60	2.41	2.18	a
$\theta_{pi,y}$	Spatial predator-prey overlap index	I	1	1	1	e
$\alpha 0_{d,i}$	Intercept for VBGF d parameter	F	-0.817	-0.375	M: -0.213 F: -0.340	d
$\alpha_{d,i,y}$	Annual intercept for VBGF d	F				
$\beta_{d,i}$	Temperature covariate for VBGF d	F	0.009	0.004	M: -0.0057 F: -0.0115	d
K_i	VBGF energy loss (kg kg^{-1} yr^{-1})	F	0.22	0.45	M: 1.08 F: 0.38	d
H_i	VBGF assimilation (kg kg^{-d} yr^{-1})	F	16.34	9.30	M: 5.19 F: 5.90	d
$t_{0,i}$	VBGF age when $W_{ij,y}$= 0 (years)	F	0.53	-0.16	M: -1.00 F: -0.28	d
M_i^{fem}	Female natural mortality	F	NA*	0.37	0.35	c
M_i^{male}	Male natural mortality	F	NA*	0.37	0.20	c

** pollock age-specific M1 residual mortalities from the assessment were used (same values for male and females).*
a. Holsman and Aydin 2015
b. Alaska Fisheries Science Center eastern Bering Sea bottom trawl survey
c. Stock assessments (Ianelli et al., 2012; Thompson and Lauth, 2012; Spies et al., 2012)
d. Tables 5 & 6
e. This assessment
f. Fishery observer data
g. Alaska Fisheries Science Center echo-integrated acoustic trawl survey
h. Juarado Molina et al., 2005

3.4 Climate informed reference points

Following Holsman et al. (2020), we use a hybrid approach to derive climate-informed ABC (Fig. 5). This includes a climate-naive target (B_{target} (i.e.,a target conditioned on historical climate) and a climate-integrated model to derive climate informed reference points (e.g., climate informed F_{target} needed to achieve x% of the species-specific climate-naive unfished biomss, B_0). This approach avoids the non-intuitive outcome of increased (decreased) harvest rates on declining (increasing) populations that arises when using climate informed targets that may be lower (higher) than present day (see Holsman et al. 2020 and Szwualski et al. 2022 for more information on this approach and issue).

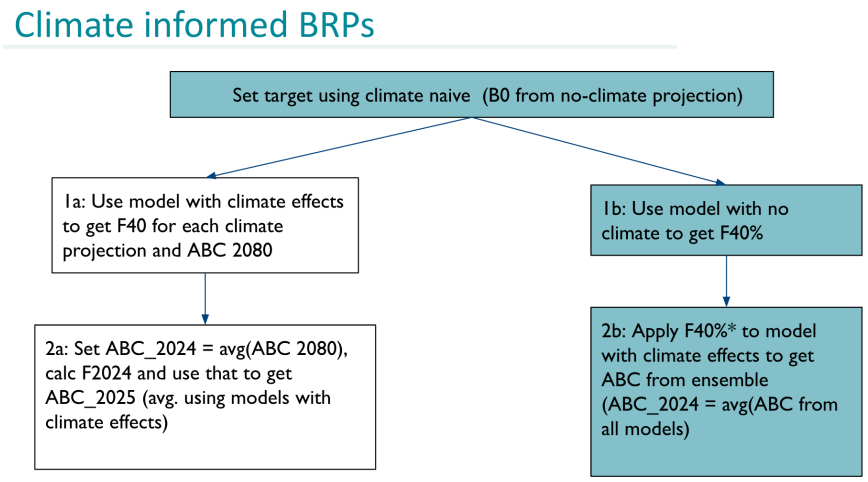

Figure 5: Based on approach of Holsman et al. 2020, stepwise approach to deriving climate naive Btarget and climate informed B status and FABC proxy. Shaded pathways indicate the approach used in this assessment.

In order to derive ABC estimates the model was projected through the year 2100 to attain relative equilibrium under a climate-naive projection (i.e., where climate is held constant in the projections at the mean of historical conditions during a climatological baseline from 1979-2010; Holsman et al., 2020, Fig. 6) without fishing (i.e.,B_0, simultaneously for pollock and Pacific cod, then for arrowtooth; Holsman et al. 2016). Using the approach of Holsman et al. (2016, 2020) and Moffitt et al. (2016), the model was then projected under fishing (with climate effects) to iteratively solve for the harvest rate (F_{target}, i.e., a climate informed rate) that results in an average of 40% of the climate-naive B_0 (i.e., $B_{40} = B_{target}$, a climate-naive target) in the last 5 years of the projection period (2094-2099), with the constraint that spawning biomass under fishing is always greater than 35% unfished biomass during the projection year; ABC_{2100} is the catch in 2100 given F_{target}. F_{target} was then applied to the model to derive ABC and F_{ABC} for 2025 to 2026 projections (Holsman et al. 2020 a,b).

3.5 Climate driven recruitment

Following Holsman et al. (2020, submitted), projections use a recruitment model with environmental covariates from the 30 layer high resolution Bering10K ROMSNPZ model hindcast(Kearney et al. 2020) and Alaska Climate Integrated Modeling (ACLIM) project projections under CMIP5 RCP45 and RCP85 and CMIP6 ssp126 and ssp585 (Hermann et al. 2021, Cheng et al. 2021, Hollowed et al. 2020). We used a combination of observed and modeled 2024 environmental conditions in the Bering Sea and estimates of SSB for each species in 2024 to predict 2025 age 1 recruitment. We modified the approach of Mueter et al. (2011) to estimate recruitment in a given year y as a function of spawning biomass and environmental covariates in the previous year *y-1*. This approach fits recruitment models with covariate effects on post-spawning survival to age 1 recruitment estimates from single- and multi- species models of CEATTLE, assuming either a linear recruitment model (i.e., no recruit per spawner effects; 'LM'), a linear model where spawning biomass is a predictor variable ('BLM'), a Ricker spawner-recruitment model, and a Beverton Holt spawner-recruitment model. Models with ROMSNPZ covariates pre-selected based on postulated relationships to spawning were included as predictors of annual variation in mean recruitment, as well as a combination of indices (where covariation in predictors < 0.5). This resulted in a set of 637 candidate models. We z-score scaled each covariate and covariates were fit to model estimates of recruitment and spawning stock biomass. We used Akaike information criterion to evaluate a set of possible candidate models with different covariate combinations, including the null model whereby no covariates were included. Recruitment models were fit using the 'futR()' package publicly available in 2024 https://github.com/kholsman/futR (see Holsman et al. submitted

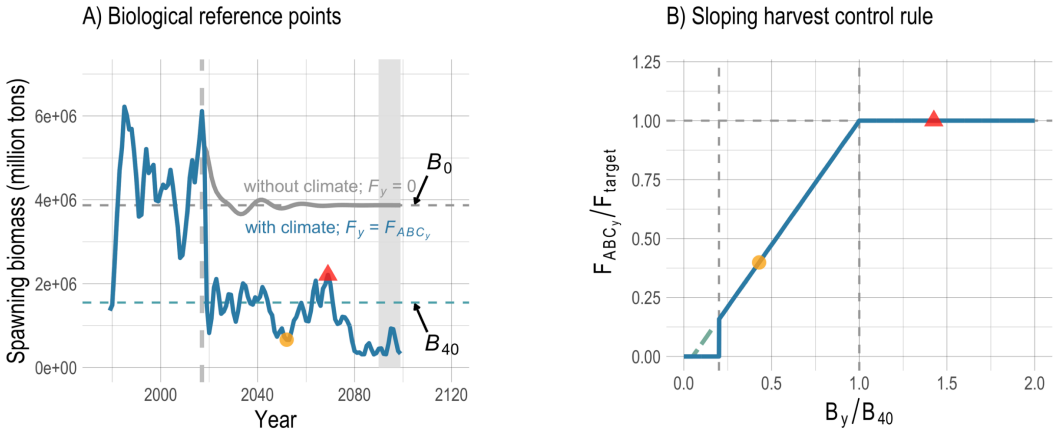

Figure 6: From Holsman et al. 2020, The climate-native unfished biomass (gray line) reference point B0 in years 2095-2099 under the persistence scenario was used to derive (Ftarget,i.e., the harvest rate that results in mean spawning target biomass in 2095-2099 equal to 40% of B0 (i.e., B40 dashed line). Climate informed By (blue line left panel) was then used to adjust FABCy lower than Ftarget if By $<$ 40% of B0 (e.g., yellow circle) using the North Pacific Fishery Management Council Tier 3 sloping harvest control rule with an ecosystem cutoff at 20% of B0 (right panel). FABCy = Ftarget when By 40% of B0 (e.g., red triangle).

for more information).

3.6 Climate-informed ABC

Here we adopted the current over fishing limit (OFL) for Tier 3 Acceptable Biological Catch (ABC) and Maximum Sustainable Yield (MSY) proxies for Bering Sea groundfish stocks; 40% of unfished biomass (SSB_0) as the proxy target biomass for the B_{ABC}, and 35% of SSB_0 as the proxy for B_{MSY} (female spawning biomass corresponding to maximum sustainable yield, MSY, i.e., 35% of ; Punt et al., 2014; NPMFC, 2013; Clark et al., 1991; Brooks et al., 2010).

The species-specific, acceptable biological catch ($\text{ABC}_{x,i,y}$) for each harvest scenario (x) was calculated as the fishery yield for each year y of the projection period $[1, n_y^{fut}]$ given a constant fishing mortality rate for the projection period that satisfies each harvest scenario objective ($F^*_{\text{ABC},x,i}$), such that:

$$\text{ABC}_{x,i,y} = \sum_{j}^{A_i}((F^*_{\text{ABC},x,i} s^{\text{f}}_{ij}/Z_{x,ij,y})(1 - e^{-Z_{x,ij,y}})N_{x,ij,y}W_{ij,y}) \tag{5}$$

where $Z_{x,ij,y}$ is the control-rule specific total annual mortality for species i age j in the set $[1, 2, \ldots A_i]$, s^{f}_{ij} is fishery age selectivity, and $N_{x,ij,y}$ and $W_{ij,y}$ are the annual species-specific abundance and weight-at-age for each projection year y. Using this approach, we found the species-specific fishing mortality rate ($F^*_{x,i}$) that results in mean female spawning biomass ($\overline{SSB}_{F,i}$) in the target projection period (i.e., last 5 years; 2046-2050) under fishing that is equal to the target proxy percentage (i.e., 40%) of mean unfished female spawning biomass ($\overline{SSB}_{0,i}$; Table 5). To find $F^*_{\text{ABC},x,i}$, we iteratively project the model to find the $\overline{SSB}_{F,i}$ that corresponds to a given harvest rate $F^*_{x,i}$, adjusting $F^*_{x,i}$ downwards if $\overline{SSB}_{F,i}$ is below the target or upwards if $\overline{SSB}_{F,i}$ is above the target, until we achieve $\overline{SSB}_{F,i}$ near or at the proxy of 40% of $\overline{SSB}_{0,i}$. We ran this harvest scenario with the following variations (sensu Holsman et al. 2020a,b):

- Project the model through the year 2100 to attain relative equilibrium under a climate-naive projection without fishing (B_0, simultaneously for pollock and Pacific cod, then for arrowtooth).
- Using the approach of Holsman et al. (2016) and Moffitt et al. (2016), the model was then projected under fishing to iteratively solve for the harvest rate (F_{target}) that results in an average of 40% of unfished biomass in the last 5 years of the projection period (2094-2099), with the constraint that spawning biomass under fishing is always greater than 35% unfished biomass during the projection years.
- F_{target} was then applied to each climate informed model under each climate scenario to derive $\text{ABC}_{target,2025}$ and $F_{ABC,2025}$ for 2025.

4 Results

4.1 Model parametrization

The multispecies mode of the model achieved a slightly higher overall fit to the data (i.e., lower negative log-likelihood with the same number of estimated parameters for both models) for pollock and similar fits to the data for Pacific cod and arrowtooth. Both models fit annual total catch for all three species closely (0.997; Fig. 7). We observed similar fits to survey biomass and age composition data from the single-species (i.e.,$\text{M2}_{ij,y}$ set to 0, hereafter single-species model) and multispecies modes of CEATTLE (Figs. 8, 26-31). Although both models predicted similar historical total and female spawning biomass, inclusion of trophic interactions in the multispecies model resulted in slightly higher estimates of total biomass for pollock (Fig. 8).

Including predation interactions in CEATTLE resulted in similar model fit to observations of survey age composition for pollock, with average annual Pearson correlation coefficient (i.e., R^2) values from CEATTLE model in multispecies mode of 0.86 versus single-species version of CEATTLE model values of 0.86 (Table 4). The single- and multispecies models performed similarly well for the annual Pacific cod and arrowtooth survey age composition data (0.64 for Pacific cod and 0.65 for arrowtooth, respectively). The single- and multispecies models fit the survey estimates of biomass with similar accuracy (single- and multispecies , R^2 respectively, of 0.49 and 0.49 for pollock, 0.48 for both models for Pacific cod, and 0.71 for arrowtooth; negative log-likelihood = 446.39, 1548.72, 692.32 and 441.47, 1565.87, 690.39 for the single- and multispecies models, respectively). Survey and fishery age selectivity curves were similar for single- and multispecies models for each species (Fig. 9).

Table 4. Correlation coefficients for 1979-2024 survey biomass and age composition data and values estimated from the model run in single-species mode (SSM) and multispecies mode (MSM).

Table 4.	*SSM*	*MSM*
Total survey biomass		
Pollock	0.49	0.49
Pacific cod	0.48	0.47
Arrowtooth	0.72	0.71
Survey age composition		
Pollock	0.85	0.86
Pacific cod	0.56	0.57
Arrowtooth	0.5	0.5

Table 5. Log likelihood equations for fitting the assessment to data sources from the fishery, summer Bering Sea groundfish survey ('GBT') or Bering Sea acoustic trawl survey ('AT') for each species i of age j in year y and where $v = 0.001$

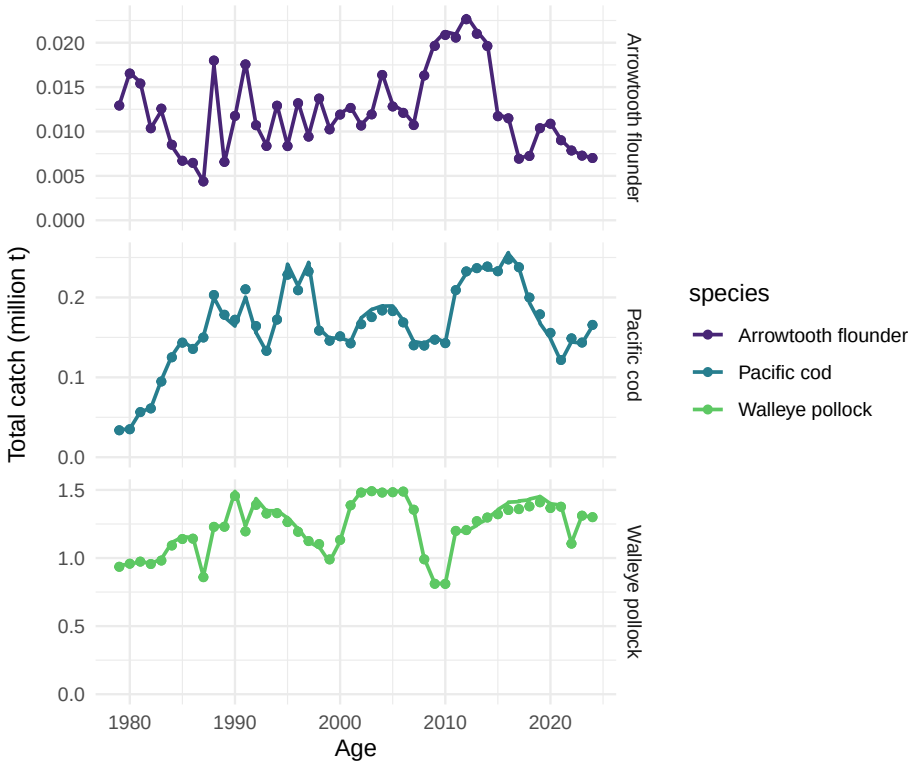

Figure 7: Total observed catch (circles) and model estimates of annual catch (lines) for single- and multispecies models (note that single species lines may not be visible as they overlap with the multispecies estimates).

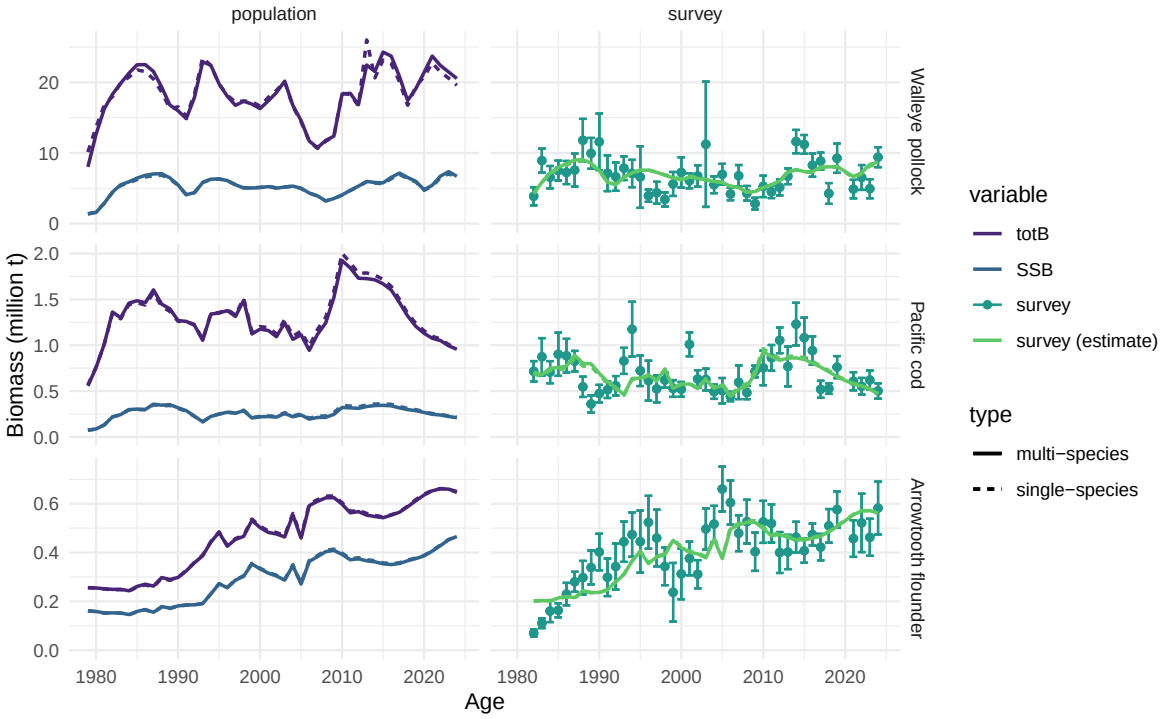

Figure 8: Single- (solid) and multispecies (dashed) retrospective model estimates of total biomass, female spawning, and measured and estimated bottom-trawl survey biomass (right hand columns). Filled circles represent mean observed groundfish survey biomass and standard errors of the mean (error bars).

Description	Equation	Data source
GBT survey biomass	$\sum_i \sum_y \frac{[\ln(\beta^s_{i,y}) - \ln(\hat{\beta}^s_{i,y}))]]}{2\sigma^2_{s,i}}$	AFSC annual Bering Sea bottom trawl survey (1979–2024), except 1979, 1980, 1981, 2020 for all three species
GBT survey age composition	$-\sum_i n_i \sum_y \sum_j (O^s_{ij,y} + v) \ln(\hat{O}^s_{ij,y} + v)$	AFSC annual Bering Sea bottom trawl survey (1979–2024), except 1979, 1980, 1981, 2020 for pollock and Pacific cod, and 1979, 1980, 1981, 2020 for arrowtooth
AT survey biomass (pollock only)	$\sum_i \sum_y \frac{[\ln(\beta^{AT}_{i,y}) - \ln(\hat{\beta}^{AT}_{i,y}))]]}{2\sigma^2_{AT}}, \sigma^2_{AT} = 0.2$	Pollock acoustic trawl survey (1979–2024)
AT survey age composition (pollock only)	$-\sum_i n_i \sum_y \sum_j (O^{AT}_{ij,y} + v) \ln(\hat{O}^{AT}_{ij,y} + v), for\ i = 1$	Pollock acoustic trawl survey (1979–2024)
Total catch	$\sum_i \sum_y \frac{[\ln(C_{i,y}) - \ln(\hat{C_{i,y}})]^2}{2\sigma^2_c}, \sigma_c = 0.05$	Fishery observer data (1979–2024)
Fishery age composition	$-\sum_i n_i \sum_y \sum_j (O^f_{ij,y} + v) \ln(\hat{O}^f_{ij,y} + v)$	Fishery observer data (1979–2024), except 2024 for pollock and 1989, 2015, 2017 for arrowtooth
Penalties		
Fishery selectivity	$\sum_i \sum_j^{A_{i-1}} x[\ln(\frac{n^f_{ij}}{n^f_{ij+1}}) - ln(\frac{n^f_{ij+1}}{n^f_{ij+2}})]^2,\ x = \begin{cases} 20, if\ \ n^f_{ij} > n^f_{ij+1} \\ 0, if\ \ n^f_{ij} \leq n^f_{ij+1} \end{cases}$	
Priors		
	$\sum_i \sum_y (\tau_{i,y})^2$ $\sum_i \sum_y (N_{0,ij})^2$ $\sum_i \sum_y (\varepsilon_{i,y})^2$	

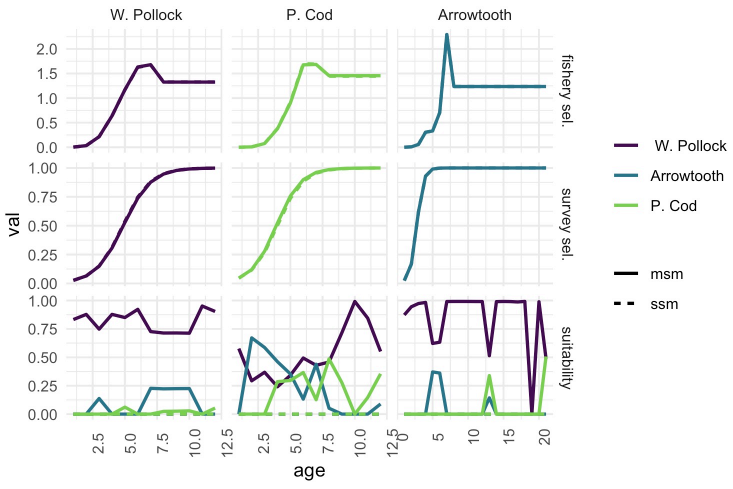

Figure 9: Single-species and multispecies fishery (first row) or survey selectivity (second row). Total suitability (across all prey species) for each predator age (third row).

4.2 Predation mortality

Implications We find evidence of continued declines in predation mortality of age 1 pollock, Pacific cod and arrowtooth flounder relative to recent high predation years (2014 - 2016). While warm temperatures continue to lead to high metabolic (and energetic) demand of predators, declines in total predator biomass, in particular Pacific cod, are contributing to an net decrease in total consumption (relative to 2016) and therefore reduced predation mortality in 2022-2024. This pattern indicates continued favorable top-down conditions for juvenile groundfish survival in 2023 through predator release due to declining biomass of groundfish.

Predation mortality has varied considerably with changes in thermal conditions and predator abundance over time (Fig. 10). While recent warm water temperatures (Fig. 2) continue to drive high individual predator demand for prey, declines in groundfish biomass combined with increased recruitment has resulted in net declines in estimates of predation mortality for juvenile groundfish in recent years. This pattern indicates continued favorable top-down conditions for juvenile groundfish survival in 2023 through 2024 via predation release. Total mortality ($M1_{ij}$+$M2_{ij,y}$) for all three species peaked in 2016 (Fig.10). Between 1980 and 1993, relatively high natural mortality rates for pollock reflect patterns in combined annual demand for pollock prey by all three predators that was high in the mid 1980's (collectively 9.87 million t per year). The peak in predation mortality of age 1 pollock in 2016 corresponds to warmer than average conditions and higher than average energetic demand of predators combined with the maturation of the large 2010-2012 year classes of pollock and Pacific cod (collectively with arrowtooth 10.62 million t per year).

At 1.42 yr^{-1}, age 1 mortality estimated by the model was greatest for pollock and lower for Pacific cod and arrowtooth, with total age 1 natural mortality at around 0.71 and 0.7 yr^{-1} for Pacific cod and arrowtooth, respectively. 2024 age 1 natural mortality across species is 12% to 38% lower than in 2016 and is near average for pollock (relative to the long-term mean) ((Fig. 10). Similarly, Pacific cod and arrowtooth age 1 mortality are well below the long-term mean.

2024 natural mortality across species is 12% to 38% lower than in 2016 and is below average for pollock (relative to the long-term mean) (Fig. 10), while Pacific cod and arrowtooth mortality rates continue to decline and are well below the long-term mean.

Temporal patterns in natural mortality reflect annually varying changes in predation mortality that primarily impact age 1 fish (and to a lesser degree impact ages 2 and 3 fish in the model). Pollock are primarily consumed by older conspecifics, and pollock cannibalism accounts for 54% (on average) of total age 1 predation mortality, with the exception of the years 2006-2008 when predation by arrowtooth marginally exceeded cannibalism as the largest source of predation mortality of age 1 pollock (Fig. 11). The relative proportion of age 1 pollock consumed by older pollock increased in 2024 relative to previous years, while the relative proportion consumed by Pacific cod and arrowtooth declined.

Patterns in the total biomass of each species consumed by all three predators in the model (typically 1-3 yr old fish) exhibit divergent trends from predation mortality in 2024. Pollock and Pacific cod biomass consumed by all predators in the model is trending upward (indicating more pollock and Pacific cod were consumed this year than in previous years), while arrowtooth consumed is trending downward (Fig. 12). Combined annual predation demand (annual ration) of pollock, Pacific cod, and arrowtooth flounder in 2024 was 8.22 million tons, down slightly from the 10.68 million t annual average during the warm years and large maturing cohorts of 2014-2016. Walleye pollock represent approximately 76% of the model estimates of combined prey consumed with a long-term average of 5.98 million tons of pollock consumed annually by all three predators in the model. From 2015 - 2019, individual annual rations were above average for all three predator species, driven by anomalously warm water temperatures in the Bering Sea during during those years. However, cooler temperatures in 2024 relative to the 2015 - 2019 warm years have resulted in annual rations at or below the long-term average (Fig. 13).

Diet analyses reveal that there are temporal shifts in the diets of juvenile and adult groundfish associated with marine heatwaves (MHW) in the region (see 2024 Ecosystem Status Report for more information). Changes in diet composition combined with temporal trends in ration (Figs. 13, 15) indicates that Pacific

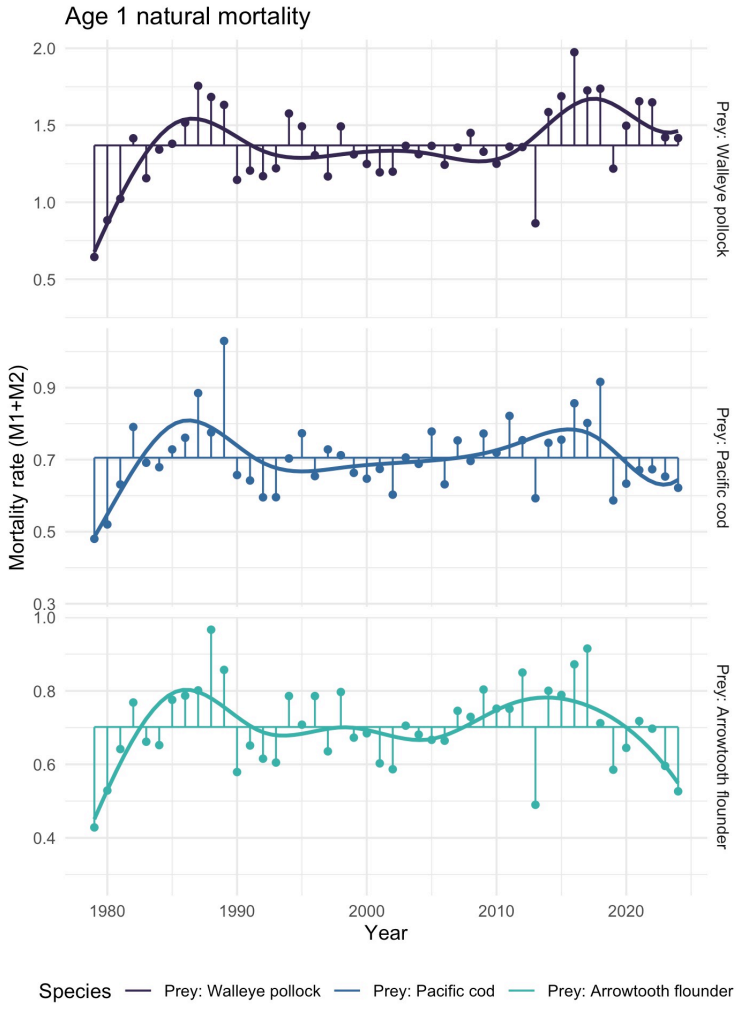

Figure 10: Annual variation in total mortality for age 1 pollock (as prey; top), age 1 Pacific cod (as prey; middle), and age 1 arrowtooth flounder (as prey; bottom) from the single-species models (dashed), and the multispecies models with temperature (points). Updated from Holsman et al. 2016. Solid lines are a 10 y (symmetric) loess polynomial smoother indicating trends in age 1 mortality over time.

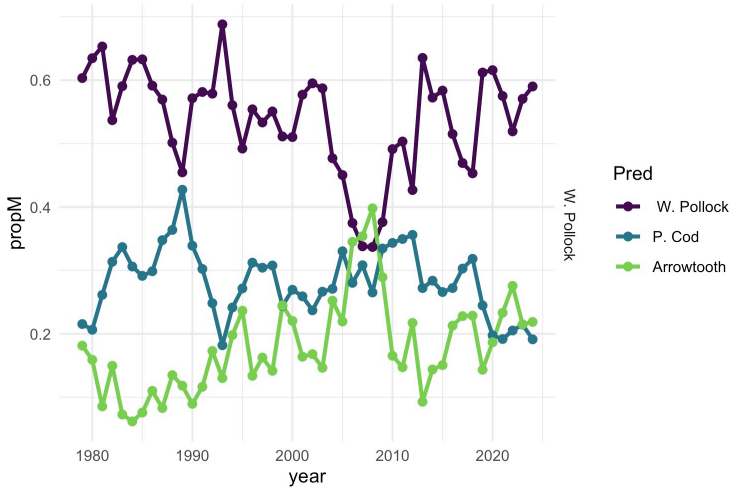

Figure 11: Proportion of total predation mortality for age 1 pollock from pollock, Pacific cod, and arrowtooth flounder predators across years.

cod consumption of pollock, Pacific cod conspecifics, and crab increased during the recent MHW (Fig. 16). Similarly, pollock consumption of zooplankton has also increased over the past decade (Fig. 16)

4.3 Biomass

- At 6.7 million tons, the 2024 EBS pollock spawning biomass from the multispecies model is above the long-term (1979-2015; a baseline that excludes years within or following unprecedented warm years) average of 5.1 million tons and represents a -9% change from 2023 and 0% change from 2022 spawning biomass levels. Similarly, the trend in total biomass observed in the past few years has continued through 2024, with recent estimates placing the total 2024 biomass (20.5 million t) above the 1979-2015 average of 17.7 million tons.
- The 2024 EBS Pacific cod female spawning biomass has declined -6% since 2023 and -12% since 2022. 2024 estimates are approximately -18% below the 1979-2015 average. Total biomass in the EBS has declined -40% since 2016, and at approximately 956 thousand tons, is 28% below the long-term 1979-2015 average of 1.3 million tons. These patterns are driven in part by continued low survey indices in 2023 and warm bottom temperatures that have induced northward redistribution of the Pacific cod stock (Spies et al. 2020, Stevenson et al. 2019).
- Arrowtooth total and spawning biomass estimates are 52% and 75% greater than the long-term 1979-2015 average (respectively), and trends suggest relatively stable biomass since 2012.
- The multispecies model estimates of a -9% and -6% change in spawning biomass (SSB) between 2023 and 2024 for pollock and Pacific cod (respectively) agree with CEATTLE single species model patterns of decline (-9% and -7%, respectively). Both models predict an increase (slightly) in spawning biomass for arrowtooth flounder relative to 2023.

4.4 Recruitment

The multispecies version of CEATTLE compensates for elevated predation mortality on younger age classes by increasing estimates of recruitment. Thus, generally recruitment is higher in the multispecies model than in the status quo single-species models for all three species, especially those with high predation rates (i.e., pollock). Here, residual mortality (M_1) for each species is adjusted in the single species (CEATTLE)

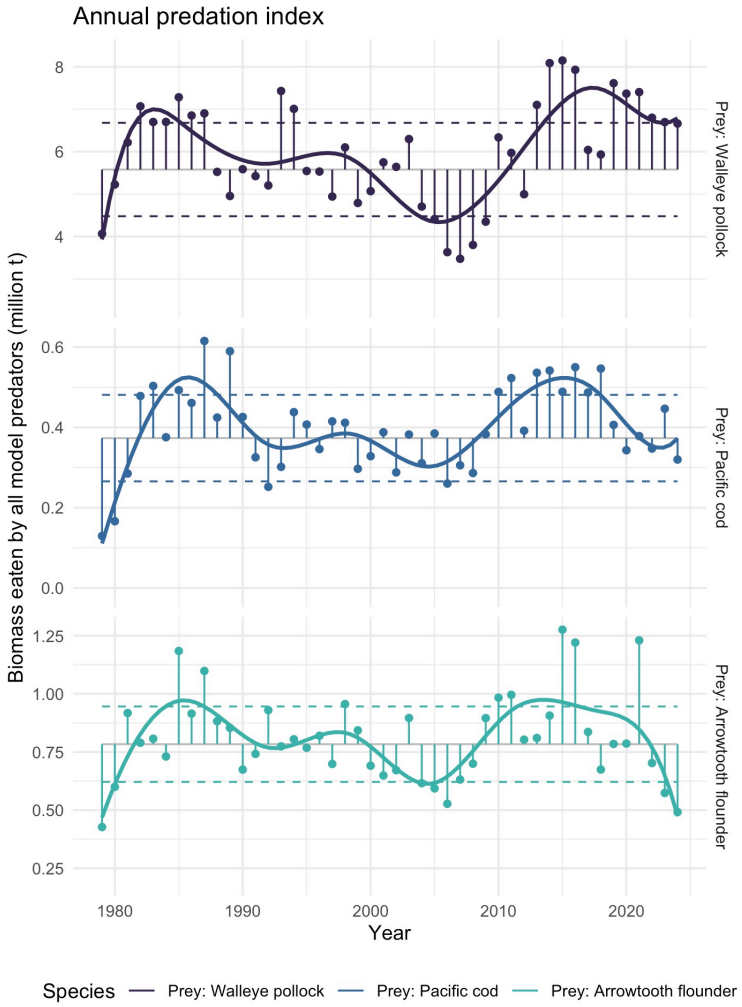

Figure 12: Multispecies estimates of prey species biomass consumed by all predators in the model (points) a) total biomass of walleye pollock consumed by predators annually b) total biomass of Pacific cod consumed by predators annually, c) total biomass of arrowtooth flounder consumed by predators annually. Gray lines indicate 1979-‘r thisYr‘ mean estimates for each species; dashed lines represent 1 standard deviation of the mean. Solid lines are a 10 y (symmetric) loess polynomial smoother indicating trends in biomass consumed over time.

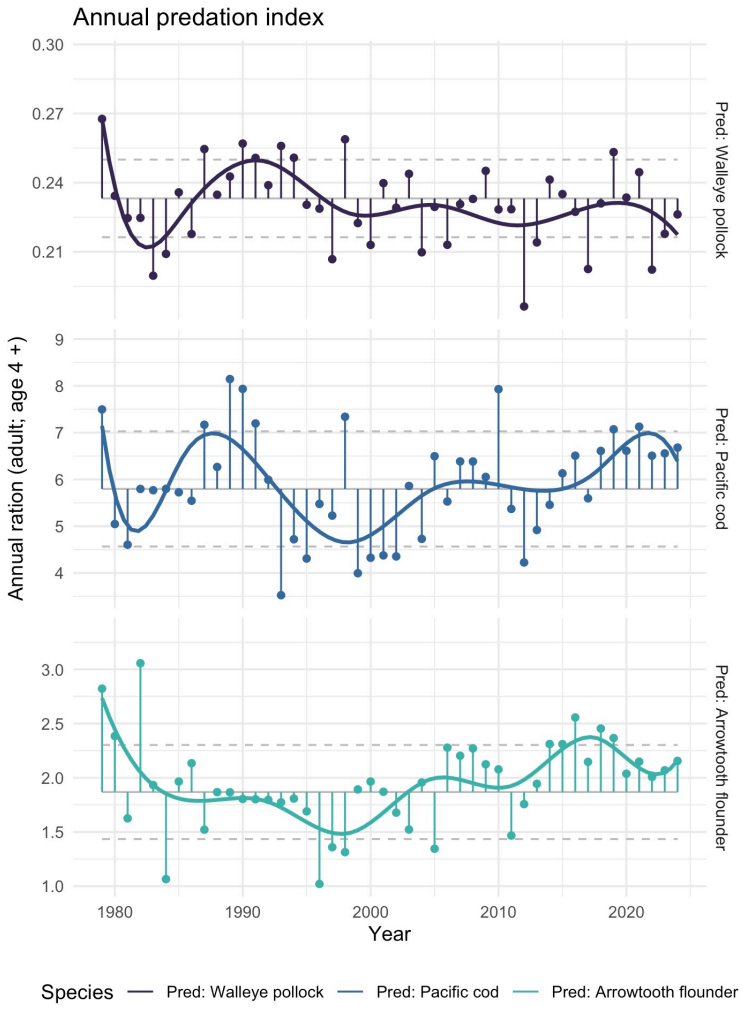

Figure 13: Multispecies estimates of annual ration (kg consumed per individual per year) for adult (age 4 +) predators: a) pollock, b) Pacific cod, and c) arrowtooth flounder. Gray lines indicate 1979 -‘r thisYr‘ mean estimates and 1 SD for each species; orange line is a 10 y (symmetric) loess polynomial smoother indicating trends in ration over time.

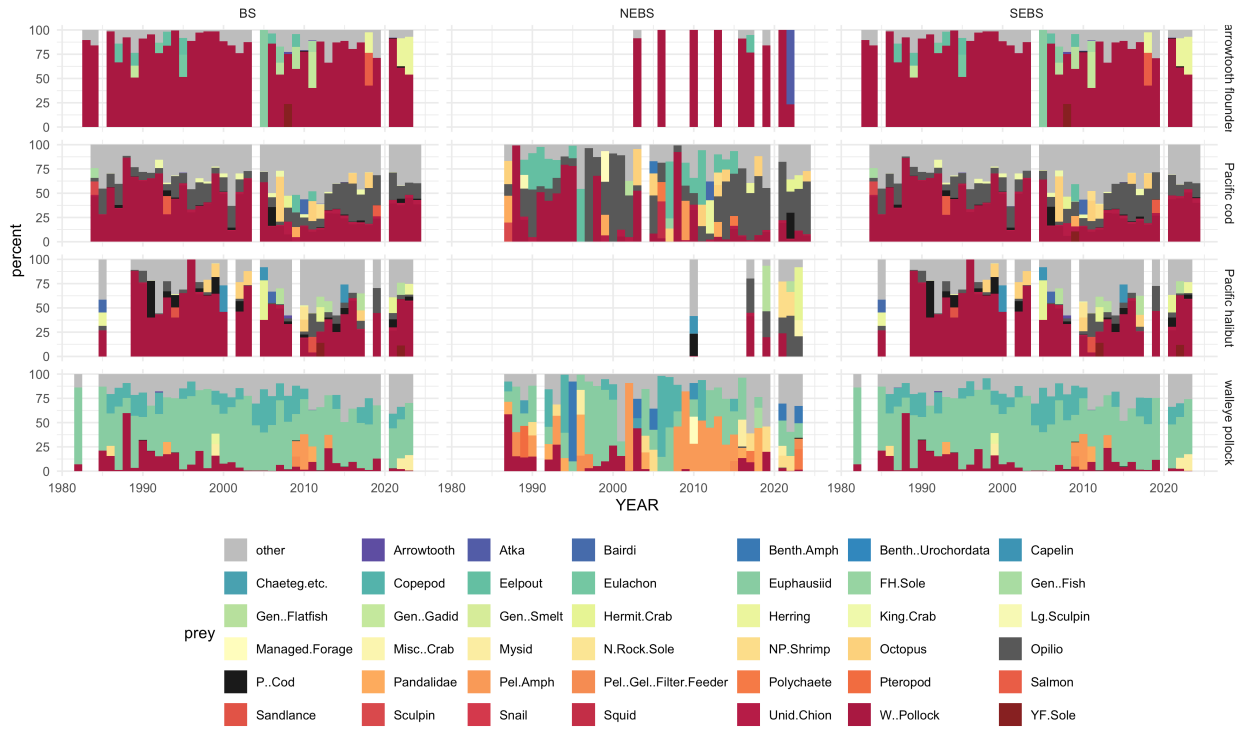

Figure 14: Average summer diet composition of adult groundfish (empirically biomass weighted by survey CPUE) for SEBS, NEBS and NEBS+ SESB combined (BS) for each predator (rows).

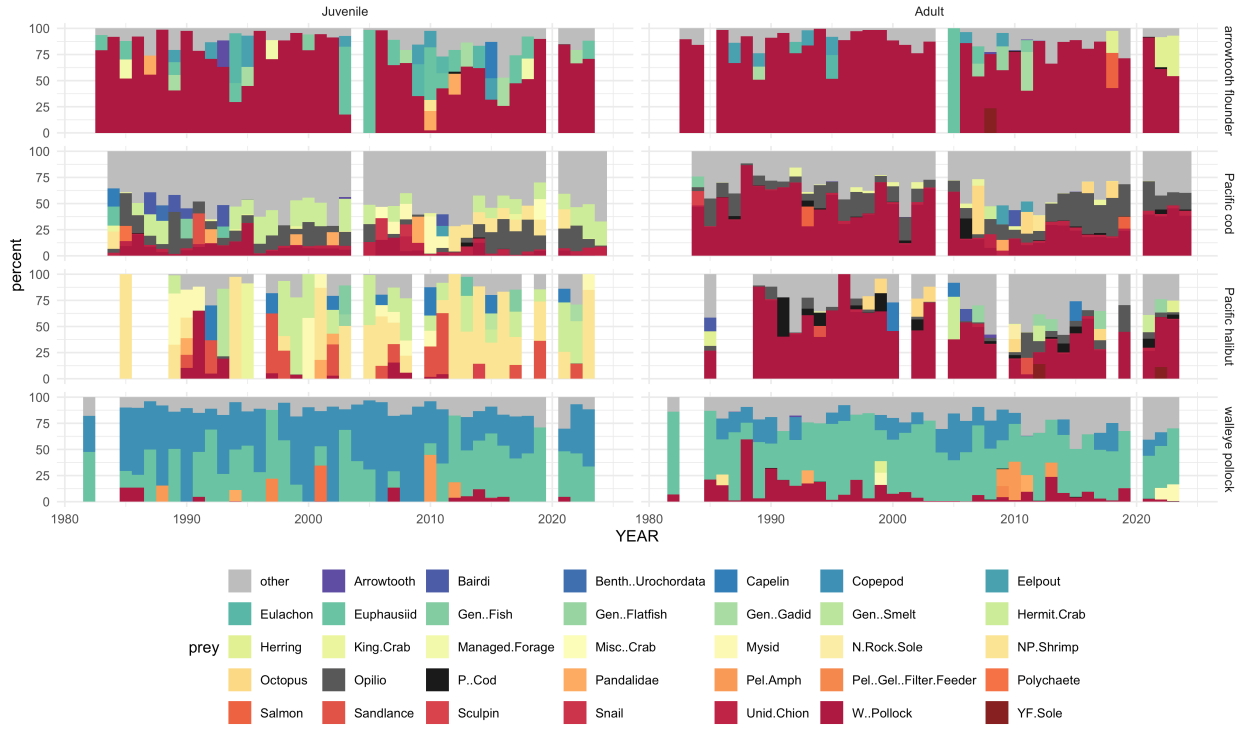

Figure 15: Average summer diet composition (empirically biomass weighted by survey CPUE) for juveniles (left column; < 45 cm) and adults (right column) of each predator (rows).

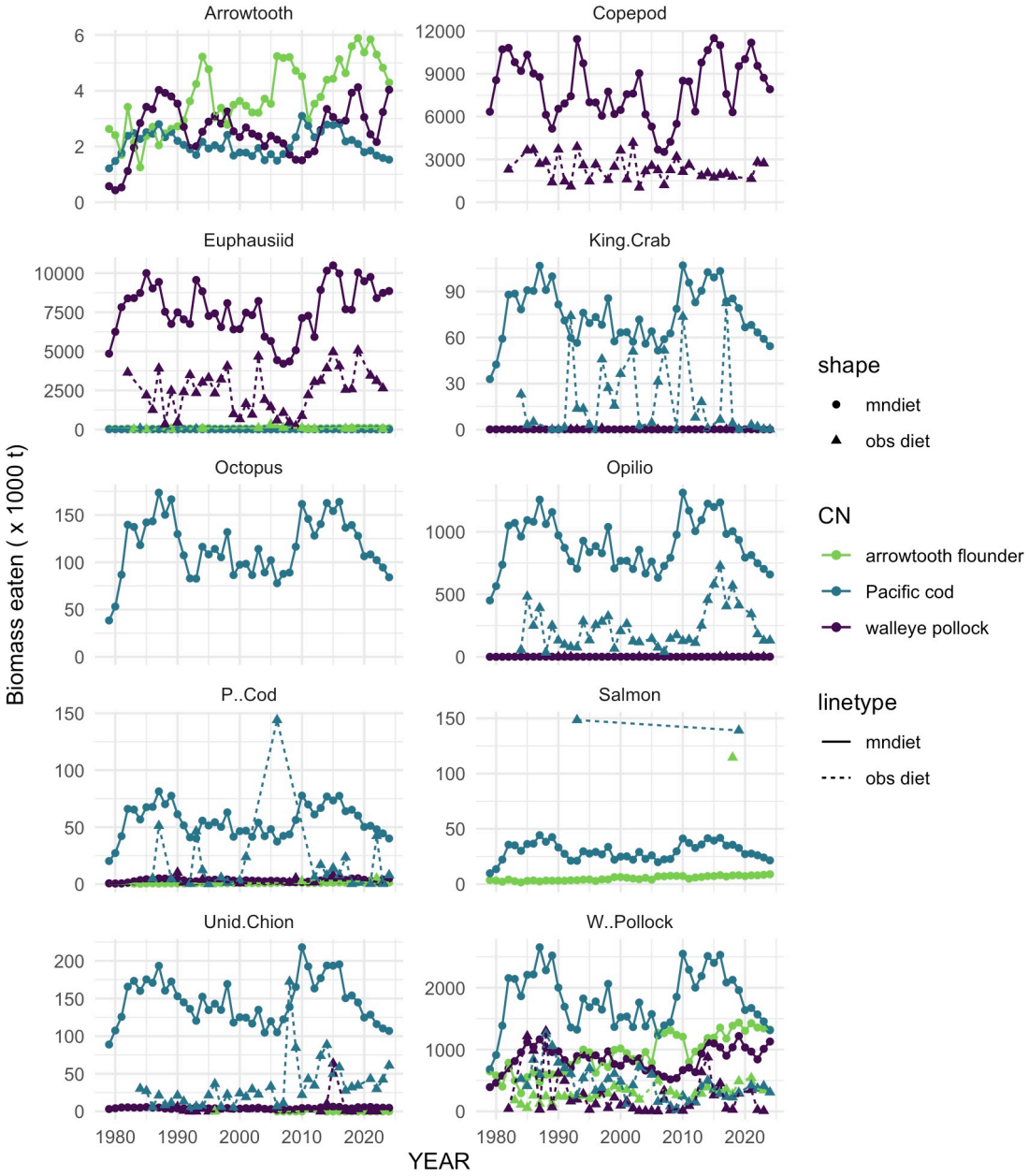

Figure 16: Patterns in prey categories consumed (panels) by each predator in the model (different colors) based on empirical annual mean diets ('obs diet' ; dashed lines; prey >50% digested removed) or averaged diets (across years) expanded by CEATTLE model estimates of annual ration (solid lines). Note that empirical diet lines where removed from arrowtooth and octopus panels; small values appox. = 1 also removed for visual clarity).

model to match the average (across years) multispecies model mortality for each age ($M_1 + M_2$). Therefore recruitment and biomass between the models is comparable (Fig. 17), although notable annual trends and productivity reference points differ. Inclusion of trophic interactions (predation) in the model resulted in slightly different stock-recruitment curves (Figs. 18, 19), with stronger density dependence for pollock in the single-species model than in the multispecies model (where density dependence would be from non-predation interactions), and peak recruitment occurring at much higher spawning biomass levels in the multispecies model (i.e., ~3.75 million tons versus ~2.5 million tons for the single species model).

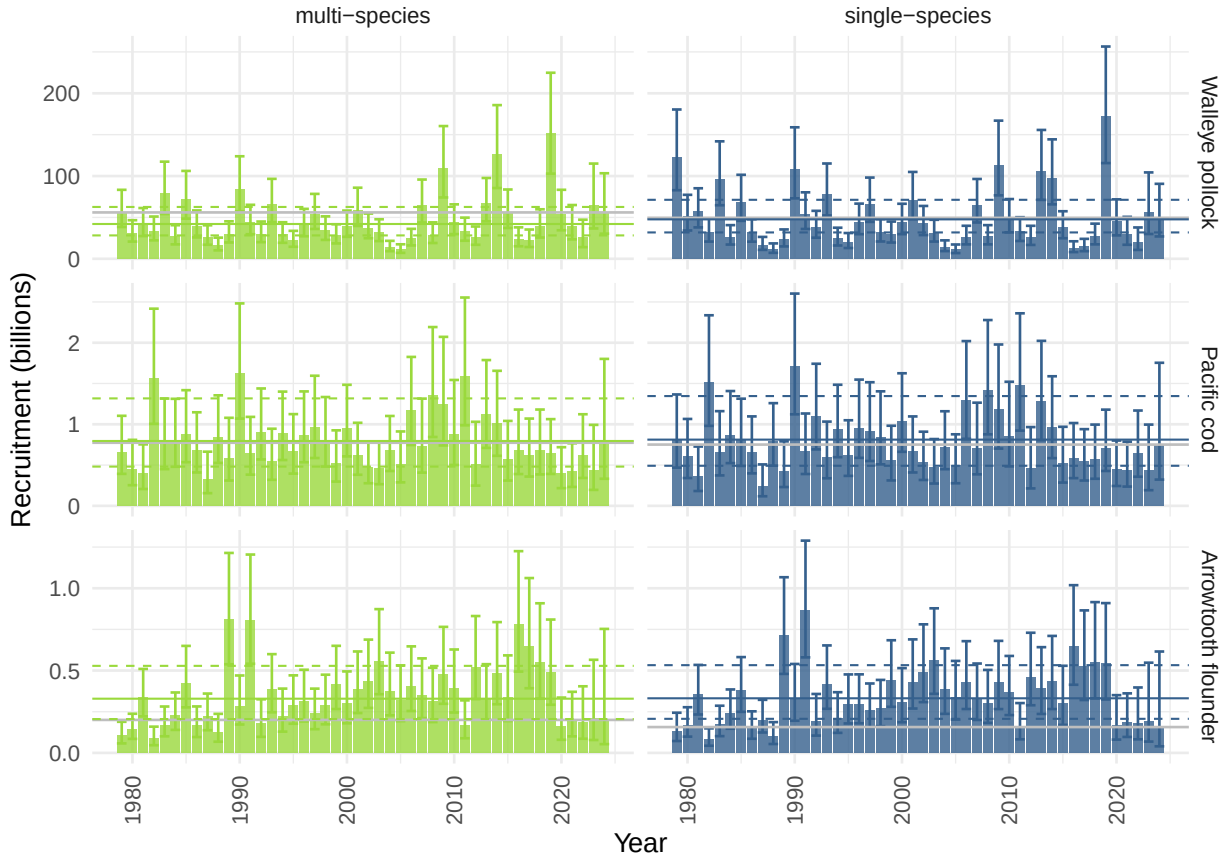

Figure 17: Annual single- and multispecies CEATTLE model estimates of recruitment (age 1) for pollock (top), Pacific cod (middle), and arrowtooth flounder (lower). Error bars represent 95% CI around mean estimates.

Although the magnitude varies between models, the overall directional change in annual recruitment estimates from year-to-year was generally the same for both models (i.e., both models increased or decreased recruitment in the same year; Fig. 17). Pollock recruitment from the single-species version of CEATTLE was slightly positively correlated with Pacific cod recruitment ($R^2 = 0.29$) and uncorrelated with arrowtooth recruitment ($R^2 = 0.06$). Correlations between pollock recruitment and Pacific cod or arrowtooth recruitment were similar between the single- and multispecies versions, although correlations were weaker in the multispecies model for Pacific cod ($R^2 = 0.19$).

Pollock age 1 recruitment estimates for 2024 are 25% above the 1979-2015 average and estimated recruitment has decreased in 2024 relative to 2023 (note that the most recent estimates have the highest uncertainty). Pacific cod age 1 recruitment in the EBS remains -5% lower than the 1979-2015 average, and is similar in 2024 to the record low recruitment estimated for 1987. Estimates of arrowtooth flounder age 1 recruitment decreased (slightly) relative to 2023 but is -40% below the 1979-2015 average.

We found some support for climate driven variation in recruitment with slightly higher support for Pacific

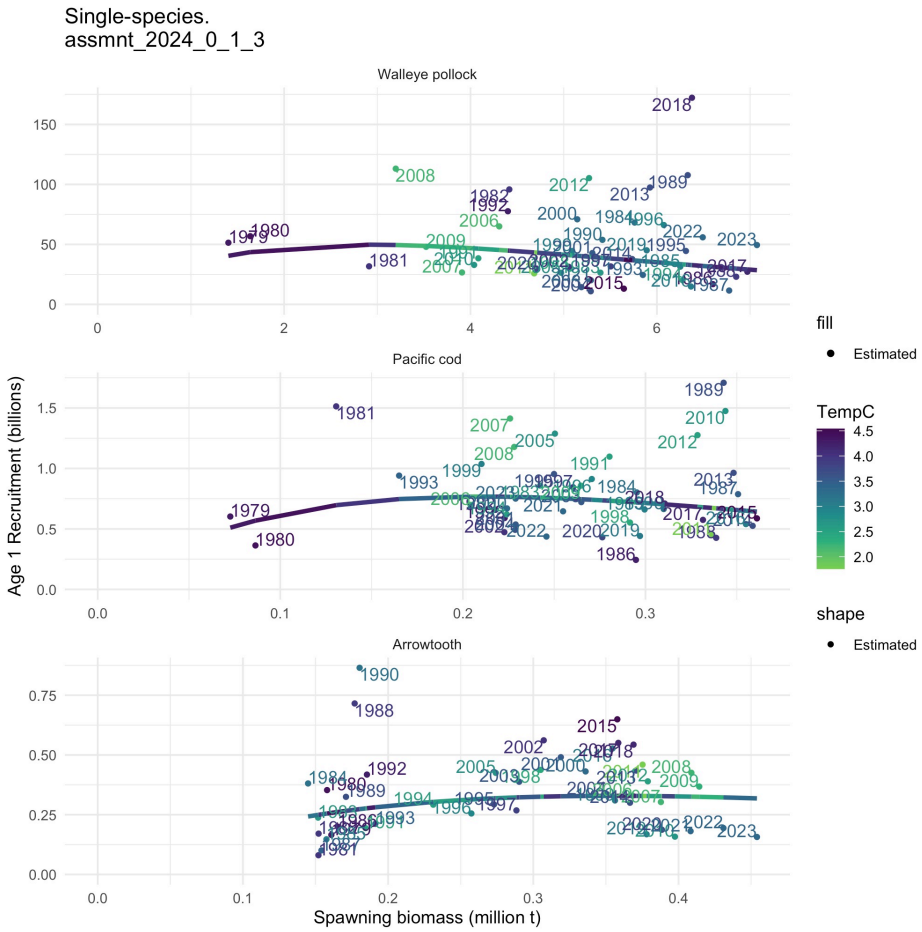

Figure 18: Spawning stock biomass and recruitment for the single-species model. Color scale text indicates cohort years summer bottom temperature (from the Bering10K ROMSNPZ model) for the EBS in deg. C. Lines represent climate-naive Ricker stock recruit curves

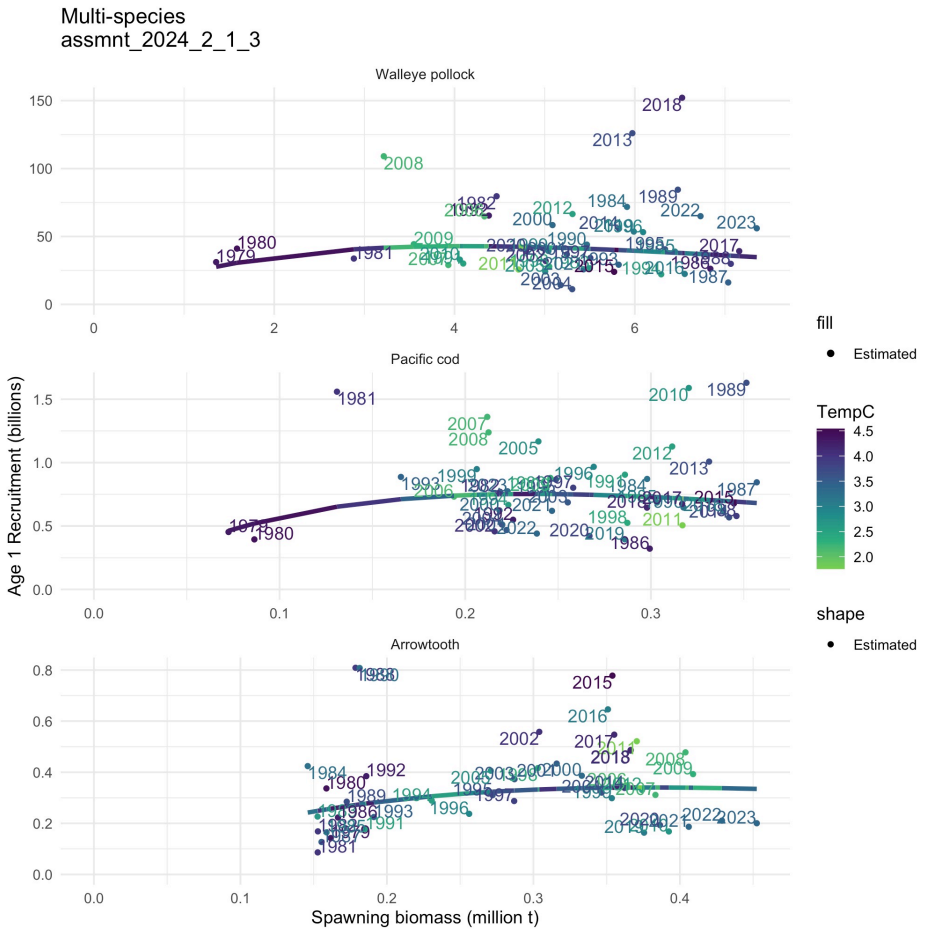

Figure 19: Spawningstock biomass and recruitment for the single-species model. Color scale text indicates cohort years summer bottom temperature (from the Bering10K ROMSNPZ model) for the EBS in deg. C. Lines represent climate-naive Ricker stock recruit curves.

Table 7: Top selected Ricker recruitment models for each species and mode.

Species	Covariates	Type	R2	deltaAIC	cumlAIC
a) Single-species					
W. Pollock	(Su)SST + (Fa)NCaS + (Sp)largeZoop	Ricker	0.4	2.476	0.3
P. Cod	(Fa)SST	Ricker	0.11	3.647	0.31
Arrowtooth	(Sp)EupS	Ricker	0.09	0	0.02
Arrowtooth	(Wi)pH + (Su)SST + (Su)BT + (Sp)largeZoop + (Fa)largeZoop	Ricker	0.25	6.631	0.92
b) Multi-species					
W. Pollock	(Su)SST + (Sp)largeZoop	Ricker	0.26	3.734	0.5
W. Pollock	(Su)SST + (Wi)EupS + (Sp)largeZoop + (Fa)largeZoop	Ricker	0.42	6.149	0.79
P. Cod	(Fa)SST	Ricker	0.1	3.149	0.35
Arrowtooth	(Wi)pH + (Sp)largeZoop + (Fa)largeZoop	Ricker	0.3	0.033	0.04
Arrowtooth	(Wi)pH + (Su)SST + (Su)BT + (Sp)largeZoop + (Fa)largeZoop	Ricker	0.31	5.635	0.82

Table 8: Top selected (all) recruitment models for each species and mode.

Species	Covariates	Type	R2	deltaAIC	cumlAIC
a) Single-species					
W. Pollock	(Su)SST + (Sp)largeZoop	Linear	0.27	0	0.03
W. Pollock	(Su)SST + (Fa)NCaS + (Sp)largeZoop	Linear, SSB(y-1)	0.42	1.389	0.14
P. Cod	(Fa)SST	Linear	0.16	0	0.07
P. Cod	(Fa)SST	Linear, SSB(y-1)	0.16	2.398	0.12
Arrowtooth	(Sp)EupS	Ricker	0.09	0	0.02
Arrowtooth	(Wi)pH + (Su)SST + (Su)BT + (Sp)largeZoop + (Fa)largeZoop	Ricker	0.25	6.631	0.92
b) Multi-species					
W. Pollock	(Su)SST + (Sp)largeZoop	Linear	0.28	0	0.03
W. Pollock	(Su)SST + (Wi)EupS + (Sp)largeZoop + (Fa)largeZoop	Linear, SSB(y-1)	0.46	4.456	0.62
P. Cod	(Fa)SST	Linear	0.13	0	0.04
P. Cod	(Fa)SST	Linear, SSB(y-1)	0.14	1.886	0.19
Arrowtooth	(Wi)pH + (Sp)largeZoop + (Fa)largeZoop	Linear	0.23	0	0.02
Arrowtooth	(Wi)pH + (Su)SST + (Su)BT + (Sp)largeZoop + (Fa)largeZoop	Ricker	0.31	5.635	0.82

cod as evidenced from a smaller set of top AICc selected models for that species (637 and 637, for single- and multi-species modes, respectively), while pollock had 637 and 637 top set of models (for single- and multi-species modes, respectively) and Arrowtooth single- and multi-species modes had 637 and 637, respectively (Tables 7,8).

Common predictor variables in the top selected recruitment models included summer and fall sea surface temperature ('(Su)SST' and '(Fa)SST'), summer bottom temperature ('(Su)BT'), fall Neocalanus ('(Fa)NCaS'), winter and spring Euphausiids ('(Wi)EupS, (Sp)EupS'), winter pH ('(Wi)pH') as well as spring and fall large Zooplankton ('(Sp)largeZoop' and '(Fa)largeZoop', respectively; Figs. 21, 22). This is consistent with previous studies that used a slightly different NPZ formulation (Holsman et al. 2020, Kearney et al. 2020), as well as field studies that have postulated the importance of lower trophic productivity for groundfish larval and juvenile survival in the Bering Sea (Duffy-Anderson et al. 2017). In general, recruitment was found to be inversely correlated with temperature and positively correlated with indices of ecosystem productivity (copepod and euphausiid abundance; Fig. 20).

4.5 Fishing mortality

The single- and multispecies models estimate similar fishing mortality rates for pollock that have remained relatively stable at around 0.12 since the early 1980s (Fig. 23). Both models also estimate low and relatively steady fishing mortality rates for arrowtooth flounder (i.e., ~ 0.03). Fishing mortality for Pacific cod is generally higher than pollock or arrowtooth, and varies over time (0.14-0.24). Fishing mortality for Pacific

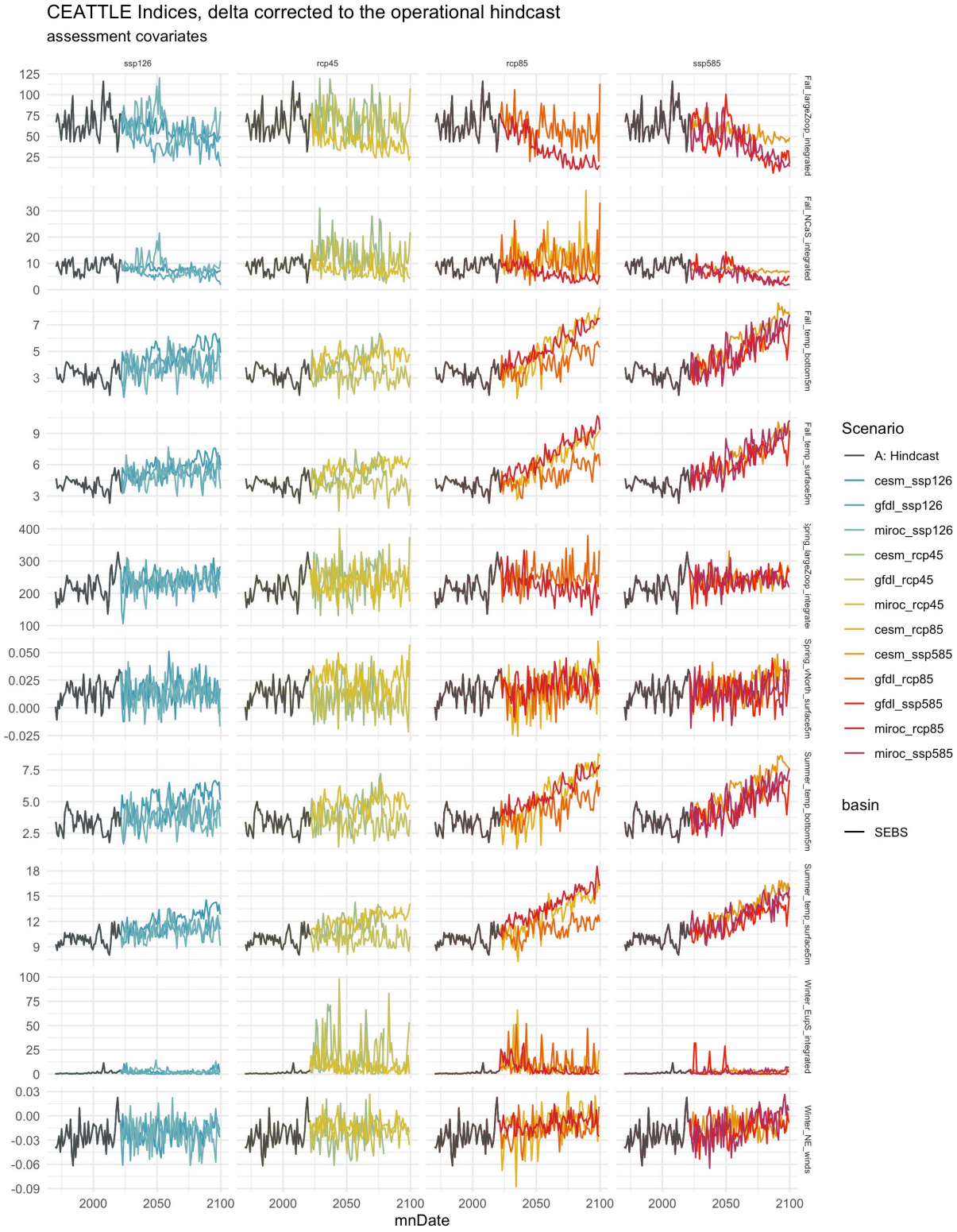

Figure 20: Candidate recruitment covariates from the Bering10K ROMSNPZ model provided through the ACLIM2 project.

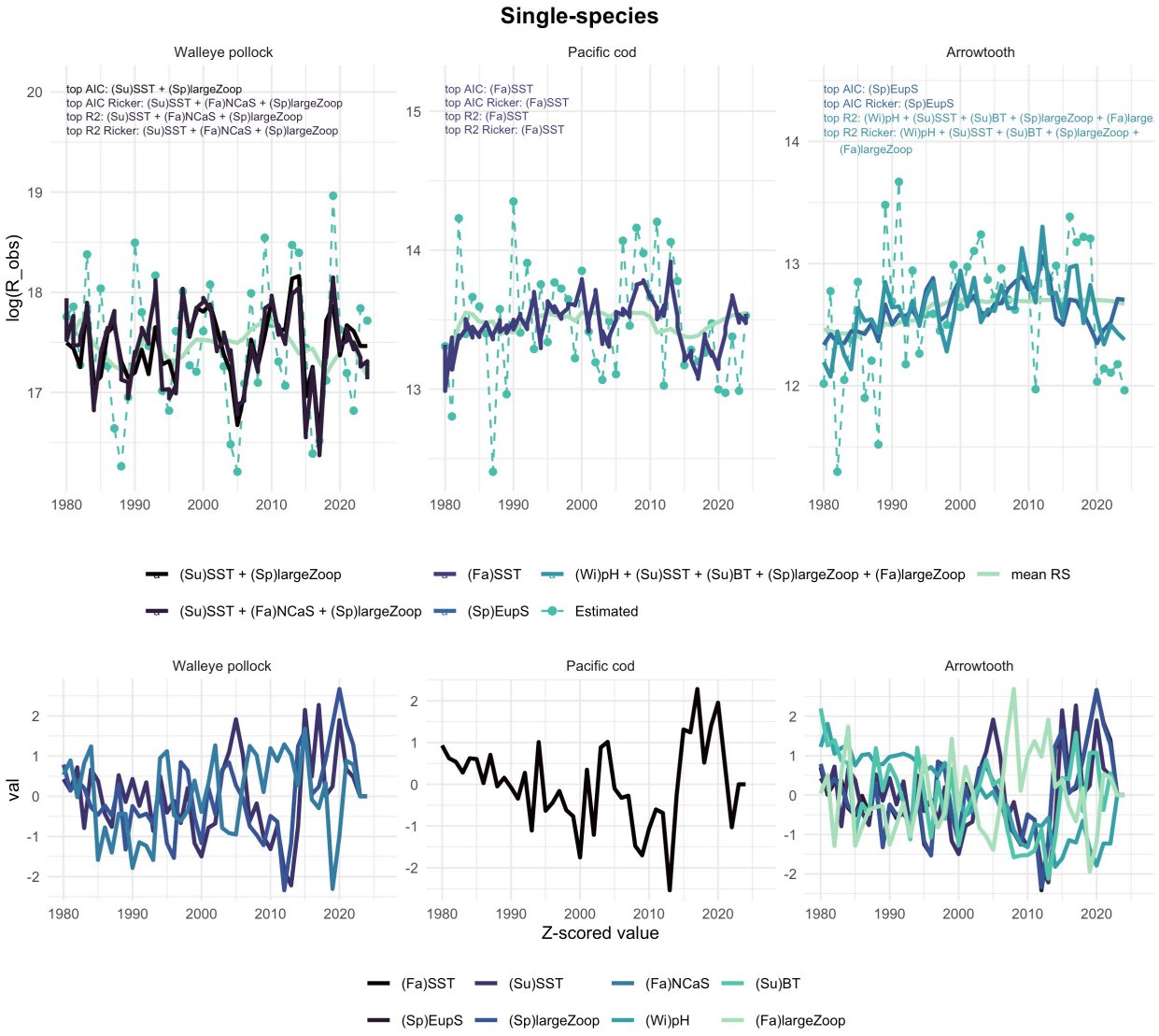

Figure 21: Recruitment covariate fits for the multispecies model updated for this year. Recruiment estimated from this year's Bering Sea CEATTLE model in single-species mode (dashed lines, top row) for each species and fits based on a climate-naive Ricker RS model, top AIC selected climate-driven model for each species, and climate-driven model with the highest R2 fit. In the bottom panel the combined covariates for the top R2 and AIC models are plotted for comparison.

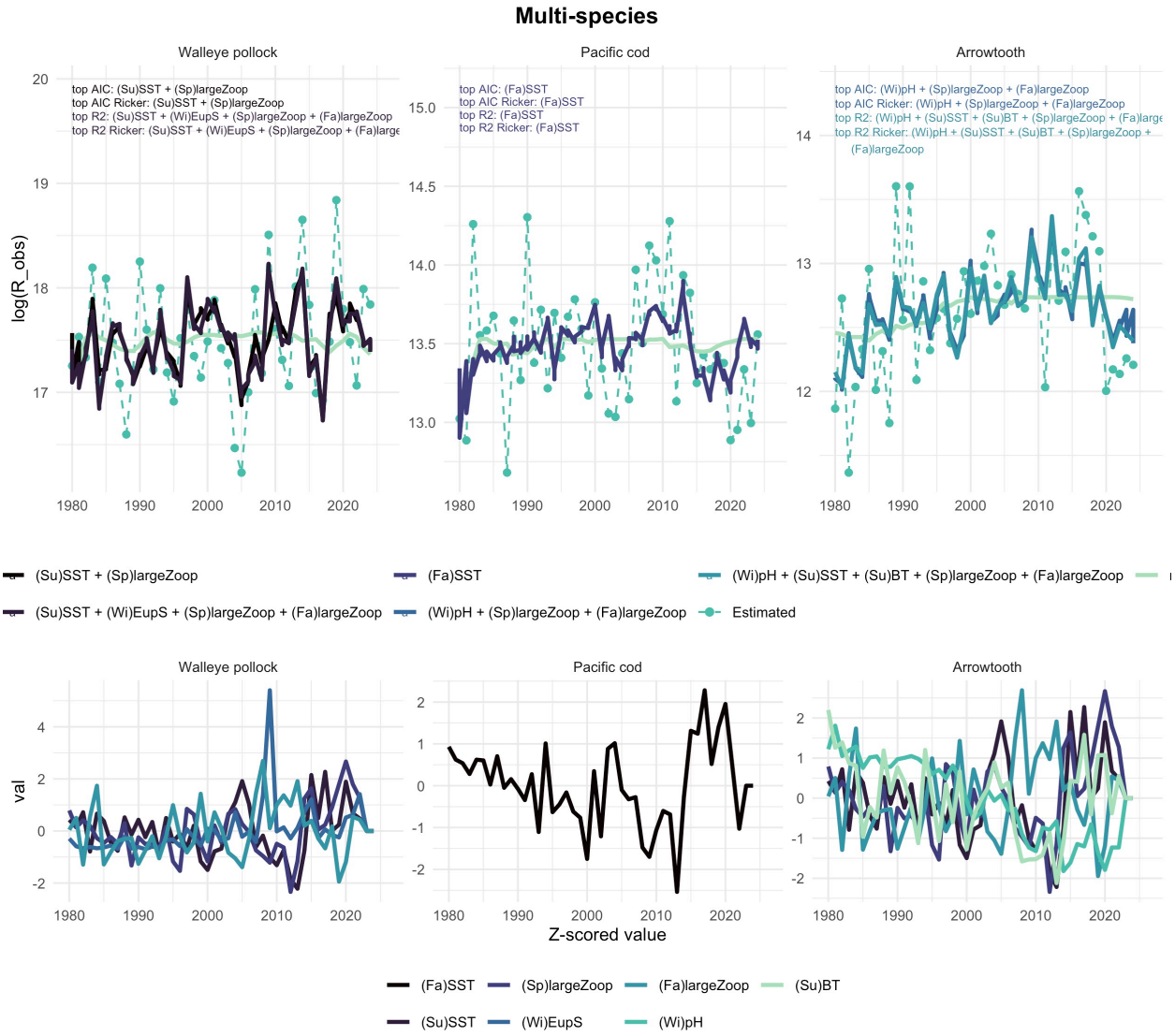

Figure 22: Recruitment covariate fits for the multispecies model updated for this year. Recruiment estimated from this year's Bering Sea CEATTLE model in multi-species mode (dashed lines, top row) for each species and fits based on a climate-naive Ricker RS model, top AIC selected climate-driven model for each species, and climate-driven model with the highest R2 fit. In the bottom panel the combined covariates for the top R2 and AIC models are plotted for comparison.

cod declined substantially between 2012-2021 with indication of slight increases in 2022-2024 (Fig. 23).

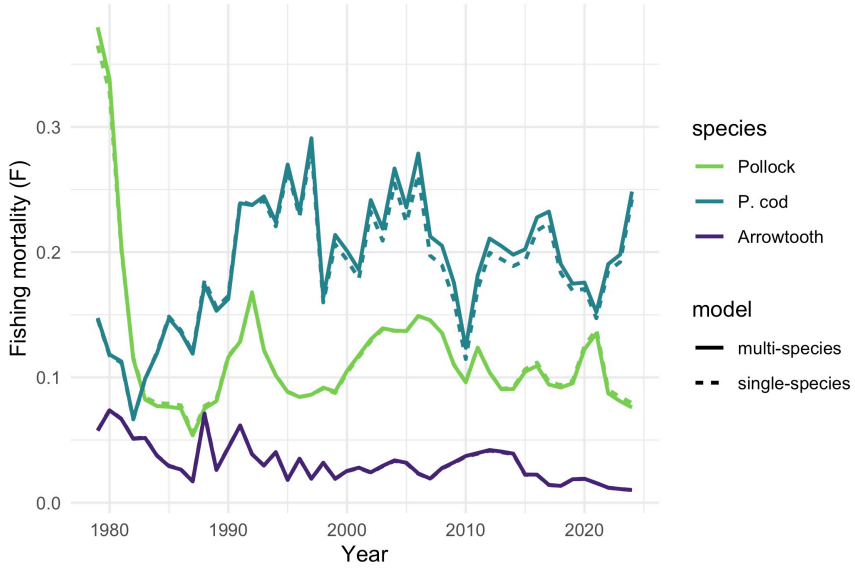

Figure 23: Timeseries of single- and multispecies (solid and dashed lines, respectively) CEATTLE model estimates of fishing mortality rate for eastern Being Sea walleye pollock, Pacific cod, and arrowtooth flounder. Note that the single- and multispecies lines for pollock and arrowtooth flounder overlap.

4.6 Climate-informed reference points

Projecting the CEATTLE model forward under environmentally driven recruitment produces trajectories of female spawning stock biomass that can be used to derive multispecies biological reference points and attendant fishing mortality rates (Holsman et al. 2016). Projections under the Ricker spawner-recruit model (without environmental effects on recruiment) lead to some over-compensation recruitment dynamics for pollock in the first years of the projection (especially for single-species models; Fig. 24; sensu Botsford, 1986). However, a >70 year projection period was sufficient to allow such dynamics to reach a relative equilibrium (Figs. 32, 33).

In general, projected unfished and harvested female spawning stock biomass ($SSB_{0,iy}$ and SSB_{target} , respectively) were similar for projections of the multi- and single-species models (Figs. 32-35) due to adjusted age 1 M_1 values for the single species model that match the mean (across years) age 1 M_2 from the multispecies model. Relative to 2024 levels, the model projects SSB of pollock will decline in 2025 (projected based on 2024 catch) followed by an decline in SSB in 2026 (projected with $F_{i,y}$ set to the climate naive $F_{target,i}$) for each species i. For Pacific cod the model projects a decline (slightly) in SSB in both 2025 and 2026.

Near-term estimates of changes in spawning biomass were generated using the climate-integrated model, where environmental covariates drive recruitment, growth, and when in multispecies mode, predation mortality. For the multispecies model, ensemble projections using climate-enhanced Ricker recruitment models and projected future warming scenarios (including low carbon mitigation/ high warming, moderate mitigation and warming, high mitigation / low warming, as well as persistence scenarios and assuming 2024 catch for 2025 and F_{ABC} for 2026) estimate a 95% chance that pollock SSB will remain between 92-95% of 2024 SSB in 2025 and will be between 79-82% of 2024 SSB levels in 2026. Ensemble projections using climate-enhanced recruitment models based on long-term projections estimate a 95% chance that Pacific cod SSB will continue to decline to between 93-98% of 2024 SSB in 2025 and between 75-78% of 2024 SSB levels in 2026. Ensemble projections using climate-enhanced recruitment models based on long-term projections estimate a 95% chance that arrowtooth SSB will be between 82 and 93% of 2024 SSB in 2025 and will be between 77 and 86% of 2024 SSB levels in 2026.

Similarly, for the single-species model, ensemble projections using climate-enhanced recruitment models and projected future warming scenarios (including low carbon mitigation/ high warming, moderate mitigation and warming, high mitigation / low warming, as well as persistence scenarios and assuming 2024 catch for 2025 and F_{ABC} for 2026) estimate a 95% chance that pollock SSB will remain between 91-95% of 2024 SSB in 2025 and will be between 82-85% of 2024 SSB levels in 2026. Ensemble projections using climate-enhanced recruitment models based on long-term projections estimate a 95% chance that Pacific cod SSB will continue to decline to between 93-98% of 2024 SSB in 2025 and between 77-81% of 2024 SSB levels in 2026. Ensemble projections using climate-enhanced recruitment models based on long-term projections estimate a 95% chance that arrowtooth SSB will be between 82 and 93% of 2024 SSB in 2025 and will be between 78 and 87% of 2024 SSB levels in 2026.

4.7 ABC and harvest recommendations

4.7.1 2024 BRP summary table (for reference only; not used for offical harvest recommendation)

As estimated or recommended this year (2024) for:

Quantity	Walleye pollock		Pacific cod		Arrowtooth flounder	
	SSM	MSM	SSM	MSM	SSM	MSM
2024 M (age 1)	1.369	1.417	0.706	0.622	0.702	0.527
2024 Average 3+ M	0.31	0.31	0.38	0.38	0.228	0.228
Projected (age 3+) B_{2025} (t)	15,873,816	16,753,272	800,824	799,099	618,934	623,892
SSB_{2024} (t)	6,444,240	6,696,310	213,889	208,936	466,348	465,848
% change in SSB (t) from 2023	-8.9	-8.9	-6.5	-6.2	2.7	3.0
Projected SSB_{2025} (t)	5,966,920	6,244,780	202,567	198,588	409,521	409,972
Projected SSB_{2026} (t)	5,372,410	5,354,810	166,917	158,785	386,437	385,489
*Projected $SSB_{0,2100}$ (t)	6,116,402	5,266,954	458,791	453,032	380,920	395,140
*Projected $SSB_{target,2100}$ (t)	2,730,110	2,838,336	215,372	204,706	152,326	157,992
**Target 2100 B/B_0	0.446	0.539	0.469	0.452	0.4	0.4
$F_{target,2100}$	0.383	0.564	0.272	0.311	0.08	0.089
$F_{ABC,2025}$	0.135	0.181	0.332	0.376	0.029	0.034
ABC_{2025}	1,955,710	2,678,690	199,816	216,098	17,979	20,751
ABC_{2026}	1,570,120	2,038,380	170,505	180,108	15,599	17,960

* $SSB_{0,2100}$ and $SSB_{target,2100}$ are based on climate-naive model projections of SSB at 2100 (equilibrium) given $F = 0$ and $F = F_{target}$, respectively.
** *Target ratios in 2100 are based on* B/B_0=0.4, given that $B/B_0 > 0.35$ for all future yr.
*** *Projected* SSB_{2025} (t) refers to SSB at the start of 2025 and Projected SSB_{2026} (t) refers to SSB at the start of 2026 using $F_{ABC,2025}$ for 2025

2023 Values

Quantity	Walleye pollock		Pacific cod		Arrowtooth flounder	
	SSM	MSM	SSM	MSM	SSM	MSM
2023 M (age 1)	1.313	1.195	0.653	0.594	0.658	0.468
2023 Average 3+ M	0.306	0.306	0.38	0.38	0.227	0.227
Projected (age 3+) B_{2024} (t)	15,860,694	16,265,727	679,301	686,562	566,160	569,909
SSB_{2023} (t)	6,790,160	7,044,480	157,340	155,597	429,700	428,256
% change in SSB (t) from 2022	10.3	10.3	-9.2	-9.0	0.1	0.2
Projected SSB_{2024} (t)	6,239,390	6,475,040	156,408	155,652	374,227	373,806
Projected SSB_{2025} (t)	5,828,060	5,819,550	128,478	123,214	351,317	348,509
*Projected $SSB_{0,2100}$ (t)	6,164,698	6,504,694	322,907	372,244	368,306	426,212
*Projected $SSB_{target,2100}$ (t)	3,044,850	3,136,376	164,934	169,131	147,286	170,536
**Target 2100 B/B_0	0.494	0.482	0.511	0.454	0.4	0.4
$F_{target,2100}$	0.345	0.547	0.443	0.481	0.08	0.086
$F_{ABC,2024}$	0.134	0.192	0.498	0.566	0.033	0.042
ABC_{2024}	2,054,020	2,965,510	188,498	205,756	17,411	21,741
ABC_{2025}	1,853,370	2,521,900	156,934	165,274	16,533	20,573

In order to derive ABC estimates, the model was projected through the year 2100 to attain relative equilibrium under a climate-naive projection without fishing (B_0, simultaneously for pollock and Pacific cod, then for arrowtooth). Using the approach of Holsman et al. (2016, 2020) and Moffitt et al. (2016), the model was then projected under fishing to iteratively solve for the harvest rate (F_{target}) that results in an average of 40% of the climate-naive unfished biomass in the last 5 years of the projection period (2094-2099), with the constraint that spawning biomass under fishing is always greater than 35% unfished biomass during the projection years. F_{target} was then applied to the model to derive ABC and F_{ABC} for 2025 to 2026 projections (Holsman et al. 2020 a,b).

The hybrid approach (i.e., climate-naive target and climate-informed status and projections) method for estimating F_{target} resulted in a proxy ABC harvest rate at equilibrium that corresponds to about 45% SSB_0 for pollock, 47% for Pacific cod, and 40% for arrowtooth flounder for single species models, and about 54%, 45%, and 40% SSB_0 for pollock, Pacific cod, and arrowtooth flounder using the multispecies model.

- Single and multispecies CEATTLE models project changes in 2025 recommended ABC for pollock over 2024 ABC (from last year's assessment) of -5% and -10%, respectively. 2026 ABC is -24% and -31% of 2024 ABC, respectively.
- Single and multispecies CEATTLE models both project increases in 2025 recommended ABC for Pacific cod over 2024 ABC (from last year's assessment) of 6% and 5%, respectively. While, 2026 ABC is -10% and -12% of 2024 ABC, respectively.
- Single and multispecies CEATTLE models both project a decline (slightly) in 2025 recommended ABC for arrowtooth flounder 2024 ABC (from last year's assessment) of 3% and -5%, respectively. 2026 ABC is -10% and -17% of 2024 ABC, respectively.

5 Climate-informed outlook

5.1 Probability of near-term (+ 1-2 yr) biomass decline or increase

- Relative to 2024 levels, the model projects SSB of pollock will decline in 2025 (projected based on 2024 catch) followed by a decline in SSB in 2026 (projected with F_{ABC}). For Pacific cod, the model projects a decline (slightly) in SSB in both 2025 and 2026.
- Ensemble projections using climate-enhanced recruitment models and projected future warming scenarios (including high (ssp126), moderate(RCP45), and low (ssp585) carbon mitigation scenarios, as well as a persistence scenario and assuming 2024 catch for 2025 and F_{ABC} for 2026, estimate a 95% probability that pollock SSB will remain between 92-95% of 2024 SSB in 2025 and will be between 79-82% of 2024 SSB levels in 2026.
- Ensemble projections using climate-enhanced recruitment models based on long-term projections estimate a 95% chance that Pacific cod SSB will continue to decline to between 93-98% of 2024 SSB in 2025 and between 75-78% of 2024 SSB levels in 2026.
- Ensemble projections using climate-enhanced recruitment models based on long-term projections estimate a 95% chance that arrowtooth SSB will be between 82 and 93% of 2024 SSB in 2025 and will be between 77 and 87% of 2024 SSB levels in 2026.

5.2 Low warming scenarios (SSP126): probability of long-term (2034, 2050, 2080) biomass decline or increase

- Trends in biomass and recruitment under high carbon mitigation (low warming; SSP126) scenarios are very similar to near-present day. *Note that projections assume no adaptation by the species, fishery, or fishery management.* See Figures 32 and 33 for more information.

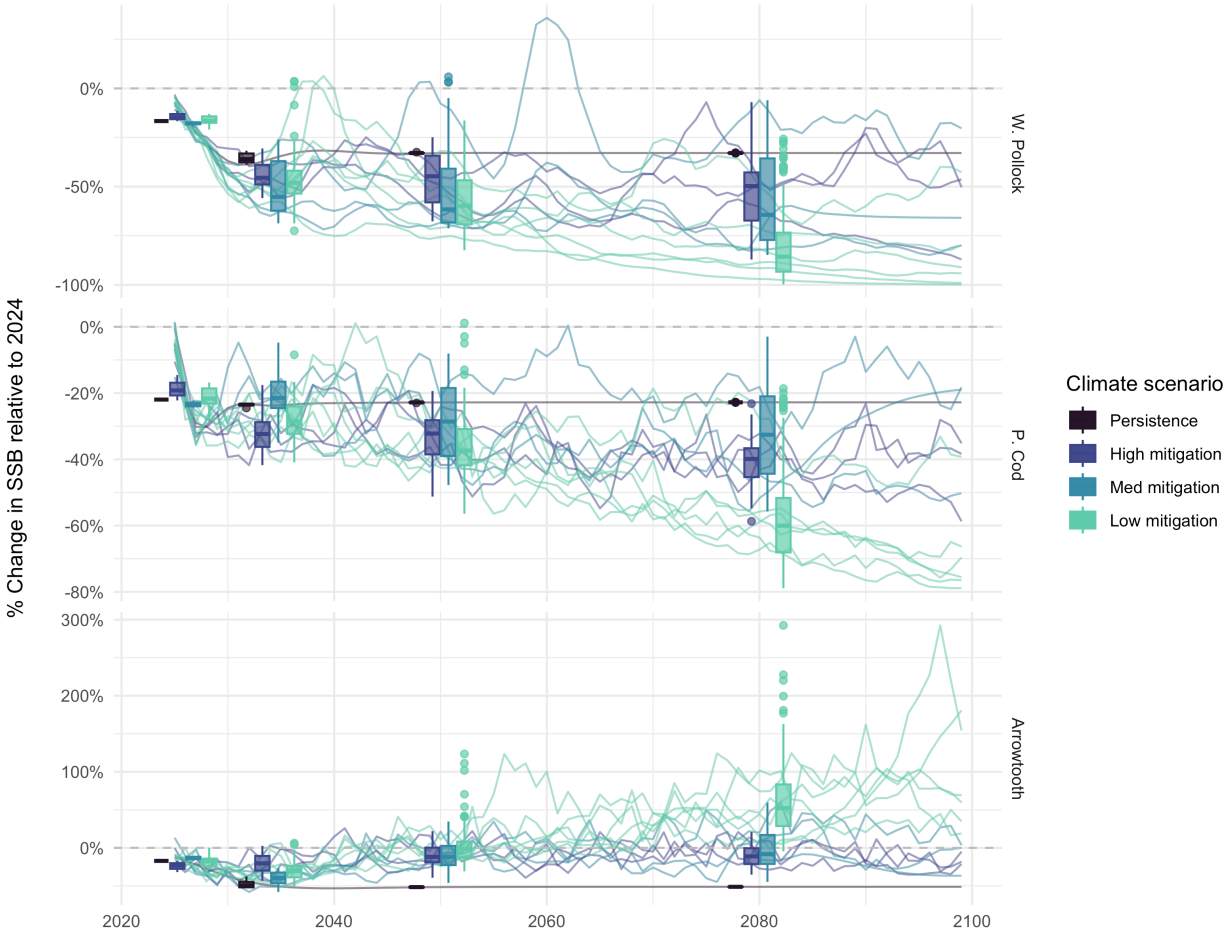

Figure 24: Climate ensemble projections of spawning stock biomass relative to this year's SSB.

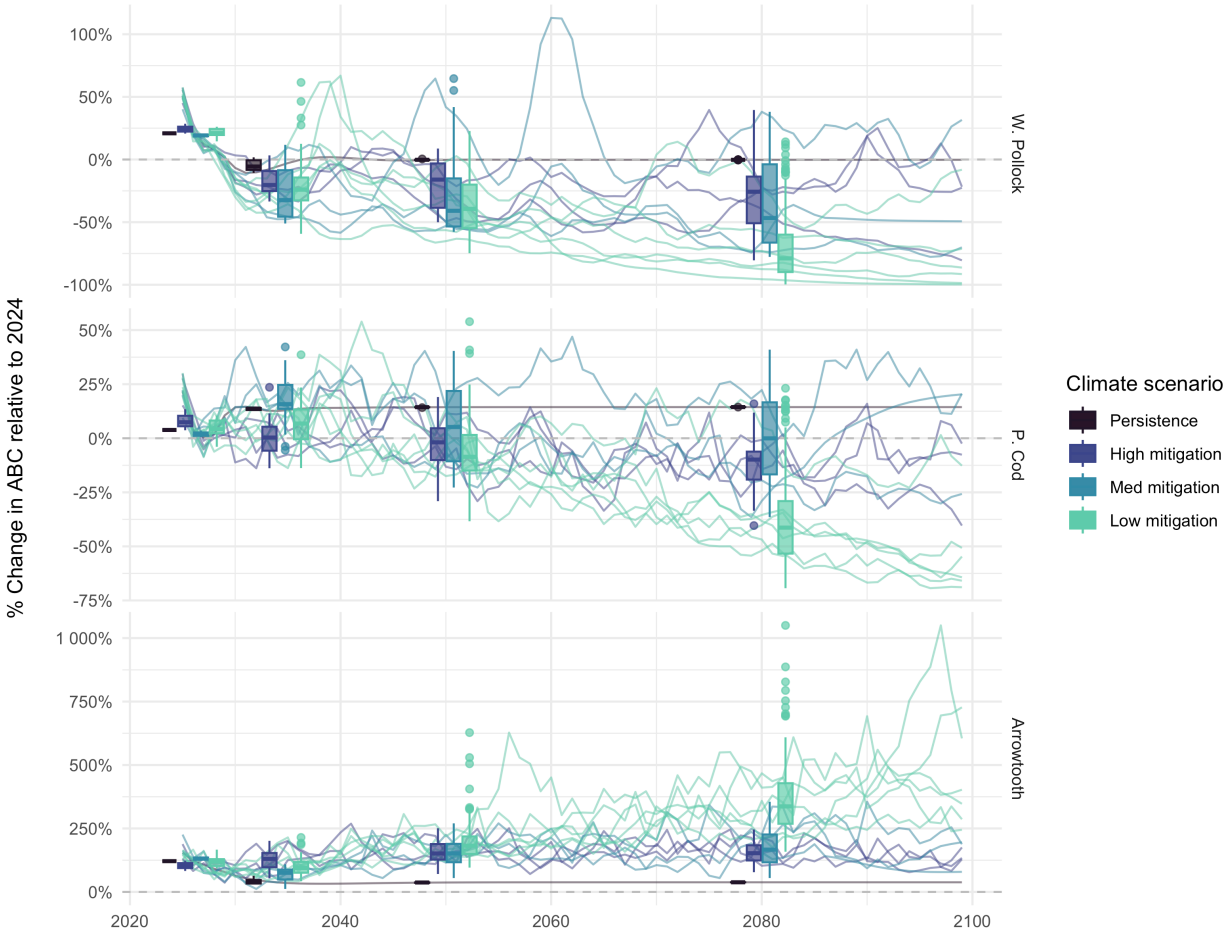

Figure 25: Climate ensemble projections of future ABC relative to this year's ABC.

- Ensemble projections using climate-enhanced recruitment models and projected future warming scenarios and assuming F_{ABC} for 2026 - 2100) estimate a 95% chance that pollock SSB will be between 58-66% of 2024 SSB in 2034, between 54-58% of 2024 SSB levels in 2050, and between 44-53% of 2024 SSB levels in 2080 (Fig. 24). Projections also estimate a 95% chance that the ABC for pollock will be between 118-131% of 2024 ABC in 2034, between 109-119% of 2024 ABC levels in 2050, and between 89-107% of 2024 ABC levels in 2080 (Fig.25).
- Ensemble projections using climate-enhanced recruitment models based on long-term projections estimate a 95% chance that Pacific cod SSB will be between 66-71% of 2024 SSB in 2034, between 66-70% of 2024 SSB levels in 2050, and between 60-63% of 2024 SSB levels in 2080. Projections also estimate a 95% chance that the ABC for Pacific cod will be between 106-116% of 2024 ABC in 2034, between 107-113% of 2024 ABC levels in 2050, and between 96-103% of 2024 ABC levels in 2080.
- Ensemble projections using climate-enhanced recruitment models based on long-term projections estimate a 95% chance that arrowtooth SSB will be between 78-106% of 2024 SSB in 2034, between 95-103% of 2024 SSB levels in 2050, and between 92-99% of 2024 SSB levels in 2080. Projections also estimate a 95% chance that the ABC for arrowtooth will be between 260-358% of 2024 ABC in 2034, between 310-339% of 2024 ABC levels in 2050, and between 300-324% of 2024 ABC levels in 2080.

5.3 High warming scenarios (SSP585): probability of long-term (2034, 2050, 2080) biomass decline or increase

- Trends in biomass and recruitment under low carbon mitigation (high warming; SSP585) scenarios are markedly different than historical or present day productivity. *Note that projections assume no adaptation by the species, fishery, or fishery management.*
- Ensemble projections using climate-enhanced recruitment models and projected future warming scenarios and assuming F_{ABC} for 2026 - 2100) estimate a 95% chance that pollock SSB will be between 70 and 105% of 2024 SSB in 2034, between 53 and 63% of 2024 SSB levels in 2050, and between 11 and 19% of 2024 SSB levels in 2080. Projections also estimate a 95% chance that the ABC for pollock will be between 140 and 212% of 2024 ABC in 2034, between 106 and 129% of 2024 ABC levels in 2050, and between 22 and 39% of 2024 ABC levels in 2080 (Figs. 24, 25).
- Ensemble projections using climate-enhanced recruitment models based on long-term projections estimate a 95% chance that Pacific cod SSB will be between 68 and 73% of 2024 SSB in 2034, between 64 and 67% of 2024 SSB levels in 2050, and between 38 and 42% of 2024 SSB levels in 2080. Projections also estimate a 95% chance that the ABC for Pacific cod will be between 111 and 120% of 2024 ABC in 2034, between 103 and 108% of 2024 ABC levels in 2050, and between 62 and 68% of 2024 ABC levels in 2080.
- Ensemble projections using climate-enhanced recruitment models based on long-term projections estimate a 95% chance that arrowtooth SSB will be between 73 and 91% of 2024 SSB in 2034, between 110 and 122% of 2024 SSB levels in 2050, and between 190 and 215% of 2024 SSB levels in 2080. Projections also estimate a 95% chance that the ABC for arrowtooth will be between 241 and 305% of 2024 ABC in 2034, between 369 and 409% of 2024 ABC levels in 2050, and between 636 and 721% of 2024 ABC levels in 2080.

6 Discussion

6.1 Application of Multispecies Biological Reference points toward climate-resilient EBFM

Development of climate-informed multispecies biological reference points (MBRPs) from climate-enhanced models like CEATTLE is a critical step in managing for climate impacts on fisheries resources (Holsman et

al. 2019; Karp et al. 2019; Link, 2010; Link and Browman, 2014). Projecting CEATTLE provides proxies for MBRPs that can readily inform current harvest advice to support Alaska fisheries management. Like previous authors, we found that ABC proxies differed from single-species CEATTLE model estimates (e.g., Gaichas et al., 2012) and are influenced by historical and future climate conditions (Holsman et al. 2020). Climate and trophic drivers can interact to affect MBRPs, but for prey species with high predation rates, trophic and management-driven changes may exceed direct effects of temperature on growth and predation in the near-term. Given this, MSCAA models can readily be used for tactical EBFM decisions under changing climate conditions, if, as suggested by Holsman et al. (2016, 2020) and others, harvest scenarios used for deriving MBRPs combined a minimum biomass threshold with yield targets to meet biodiversity and yield objectives (Worm et al., 2009; Gaichas et al., 2012). Biomass thresholds will require development of criteria for minimum limits in order represents a necessary advancement of the current approach.

6.2 Short-term utility: potential application for climate informed single species assessments

This work demonstrates some alternative applications of climate-informed multispecies trophic models within a management setting and there may be immediate relevance for current stock assessment models. For example, the estimated historical time series of natural mortality at age over time (M1 + M2) could be used directly within the assessment or used as priors in alternative assessment models with estimated age-specific and annually varying natural mortality. Similarly, for the case of EBS pollock, the climate-informed SSB and stock recruitment relationship may provide a basis for better estimates or prior distribution specification. It may be that by adding the time series of estimated total natural mortality at age that the estimated stock recruitment relationship may differ substantially given the relative differences in age 1 abundances. Further research on applying alternative stock recruitment relationships is needed as well, especially since the application of the Ricker curve has traditionally been justified due to cannibalistic nature of pollock, a situation that is partially accounted for in this application.

6.3 Long-term utility: climate- and trophic-specific biological reference points

Long-term projections of climate conditions (ideally ensembles to capture future uncertainty) are needed to inform long-term climate-specific reference points (Holsman et al. 2019), while short-term forecasts (e.g., <2 years) would also advance near-term understanding of harvest and productivity reference points, especially change in weight at age and survival within the 2 year harvest specification period (Karp et al. 2019). This assessment demonstrates the utility of using long-term projections to inform annual harvest reference points. Ongoing ROMSNPZ model validation is be useful for evaluating predictive performance and potential utility going forward. Incorporating additional species into the model, such as northern fur seals and Pacific halibut, could help provide quantitative estimates of changes in juvenile pollock forage resources associated with different harvest rates of groundfish species in the EBS, as well as refine estimates of predation mortality for prey species in the model under changing conditions. Finally, ongoing incorporation of harvest scenarios into the model will add realism to projections both for assessment purposes and for research applications.

7 Acknowledgments

Our work is the result of numerous collaborations with researchers at the University of Washington (UW), University of Alaska Fairbanks (UAF), and the NOAA Alaska Fisheries Science Center (AFSC) and Northwest Fisheries Science Center (NWFSC). We thank the Groundfish assessment, Age and Growth, Resource Ecology and Ecosystem Modeling, and Acoustics teams and programs at the AFSC, the ACLIM team, and the Bering10K modeling team for insight into this work. In particular, Ron Heintz (AFSC), Franz Mueter (UAF), and Elizabeth Siddon (AFSC) supported an excellent discussion of the bioenergetics model sub-component of CEATTLE. We thank Grant Thompson (AFSC), I. Kaplan (NWFSC), and P. Sean

McDonald (UW) for providing feedback on previous drafts. Drs. E. Moffitt and A. Punt contributed significantly to the development of multispecies harvest control rules and climate reference points used in this assessment. Support for the CEATTLE model came from the Alaska Integrated Ecosystem Assessment program (noaa.gov/iea), the NMFS Fisheries And The Environment (FATE) program, the Stock Assessment Analytical Methods program under award number 0002, and the North Pacific Research Board (publication number 547). This effort would not be possible without the help of numerous researchers and volunteers who contribute annually to the collection of biomass, demography, and diet information through Alaska Fishery Science Center surveys and the NOAA observer program, and the help of those who provide access to fishery-dependent and independent data through the Alaska Fisheries Science Center.

8 References

Adams, G. D., K. K. Holsman, S. J. Barbeaux, M. W. Dorn, J. N. Ianelli, I. Spies, I. J. Stewart, A. E. Punt (2022) An ensemble approach to understand predation mortality for groundfish in the Gulf of Alaska. Fisheries Research (251) https://doi.org/10.1016/j.fishres.2022.106303.

Botsford, L. W., 1986. Effects of environmental forcing on age-structured populations: Northern California Dungeness crab (Cancer magister) as an example. Can. J. Fish. Aquat. Sci. 43, 2345-2352.

Brooks, E. N., Powers, J. E., and Cort??s, E., 2010. Analytical reference points for age-structured models: application to data-poor fisheries. ICES J. Mar. Sci., 67, 165175.

Caddy, J. F., Mahon, R., 1995. Reference points for fishery management. FAO Fisheries Technical Paper 347.

Cheung, W.W.L., Brodeur, R. D., Okey, T. A., Pauly, D., 2015. Projecting future changes in distributions of pelagic fish species of Northeast Pacific shelf seas. Prog. Oceanogr. 130, 1931.

Clark, W. G., 1991. Groundfish exploitation rates based on life history parameters. Can. J. Fish. Aquat. Sci. 48, 734750.

Collie, J. S., Gislason, H., 2001. Biological reference points for fish stocks in a multispecies context. Can. J. Fish. Aquat. Sci. 58, 2167-2176.

Coyle, K. O., Eisner L. B., Mueter F. J., Pinchuk A. I., Janout M. A.,Cieciel, K. D., Farley, E.V., Andrew, A. G., 2011. Climate change in the southeastern Bering Sea: impacts on pollock stocks and implications for the Oscillating Control Hypothesis. Fish. Ocean. 20(2), 139156.

Curti, K. I., Collie, J. S., Legault, C. M., and Link, J. S., 2013. Evaluating the performance of a multispecies statistical catch-at-age model. . Can. J. Fish. Aquat. Sci. 70, 470-484.

Danielsson, A., Stefansson, G., Baldursson, F. M., Thorarinsson K., 1997. Utilization of the Icelandic cod stock in a multispecies context. Mar. Res. Econ. 12(4), 329-344.

Dorn, M., Aydin, K., Jones, D., Palsson, W., Spalinger, K., 2014. Chapter 1: Assessment of the Walleye Pollock Stock in the Gulf of Alaska. In Stock Assessment and Fishery Evaluation Report for the Groundfish Resources of the Gulf of Alaska Region, Alaska Fisheries Science Center, National Marine Fisheries Service, Anchorage, AK, p 53170.

Duffy-Anderson JT, Stabeno PJ, Siddon EC, Andrews AG, Cooper DW, Eisner LB, et al. (2017) Return of warm conditions in the southeastern Bering Sea: Phytoplankton - Fish. PLoS ONE 12(6): e0178955. https://doi.org/10.1371/journal.pone.0178955

Dunn, J. R. Matarese, A. C., 1987. A review of the early life history of Northeast Pacific gadoid fishes. Fish. Res. 5, 165-184.

Gaichas, S., Gamble, R., Fogarty, M., Beno??t, H., Essington, T., Fu, C., Koen-Alonso, M., Link, J., 2012. Assembly rules for aggregate-species production models: simulations in support of management strategy evaluation. Mar. Eco. Prog. Ser. 459, 275292.

Gamble R. J. and Link, J. S., 2009. Analyzing the tradeoffs among ecological and fishing effects on an example fish community: a multispecies (fisheries) production model. Ecol. Model. 220, 2570-2582.

Gamble, R. J. and Link, J., 2012. Using an aggregate production simulation model with ecological interactions to explore effects of fishing and climate on a fish community. Mar. Eco. Prog. Ser. 459, 259274, 2012 doi: 10.3354/meps09745

Gislason, H. 1999. Single and multispecies reference points for Baltic fish stocks. ICES J. Mar. Sci. 56, 571-583.

Gouhier, T. C., Guichard, F., Gonzalez, A., 2010. Synchrony and Stability of Food Webs in Metacommunities. Am. Nat., 175 (2), E16-E34

Essington, T., Kitchell J., Walters, C., 2001. The von Bertalanffy growth function, bioenergetics, and the consumption rates of fish. Can. J. Fish. Aquat. Sci. 58, 21292138.

Fogarty, M. J. 2014. The art of ecosystem-based fishery management. Can. J. Fish. Aquat. Sci. 71, 479-490.

Fogarty, M.J., Overholtz, W. J., Link, J. S., 2012. Aggregate surplus production models for demersal fishery resources of the Gulf of Main. Mar. Ecol. Prog. Ser. 459, 247-258.

Fournier, D. A., Skaug, H. J., Ancheta, J., Ianelli, J., Magnusson, A., Maunder, M. N., Nielsen, A., Sibert, J., 2012. AD Model Builder: using automatic differentiation for statistical inference of highly parameterized complex nonlinear models. Optimization Methods and Software, 27, 233-249.

Fulton, E. A., Link, J. S., Kaplan, I. C., Savina-Rolland, M., Johnson, P., Ainsworth, C., Horne, P., Gorton, R., Gamble, R.J., Smith, A.D.M., Smith, D.C., 2011. Lessons in modelling and management of marine ecosystems: the Atlantis experience. Fish Fish. 12, 171188.

Hanson, P., Johnson, T. Schindler, D., Kitchell, J., 1997. Fish Bioenergetics 3.0. Madison, WI: University of Wisconsin Sea Grant Institute.

Hamre, J. 2003. Capelin and herring as key species for the yield of north-east Arctic cod. Results from multispecies model runs. Sci. Mar. 67 (Suppl 1), 315-323.

Hermann et al., 2021 A.J. Hermann, K. Kearney, W. Cheng, D. Pilcher, K. Aydin, K.K. Holsman, et al. Coupled modes of projected regional change in the Bering Sea from a dynamically downscaling model under CMIP6 forcing Deep-Sea Res. II (2021), 10.1016/j.dsr2.2021.104974 194 104974.

Hollowed, K. K. Holsman, A. C. Haynie, A. J. Hermann, A. E. Punt, K. Y. Aydin, J. N. Ianelli, S. Kasperski, W. Cheng, A. Faig, K. Kearney, J. C. P. Reum, P. D. Spencer, I. Spies, W. J. Stockhausen, C. S. Szuwalski, G. Whitehouse, and T. K. Wilderbuer. Integrated modeling to evaluate climate change impacts on coupled social-ecological systems in Alaska. Frontiers in Marine Science, 6(January):1–18, 2020. DOI: 10.3389/fmars.2019.00775.

Hilborn, R. and Walters, C. J., 1992. Quantitative Fisheries Stock Assessment: Choice, Dynamics and Uncertainty. Chapman and Hall, New York. 570 p.

Hollowed, A. B., Bax, N., Beamish, R., Collie, J., Fogarty, M., Livingston, P., Pope, J., Rice, J. C., 2000a. Are multispecies models an improvement on single-species models for measuring fishing impacts on marine ecosystems? ICES J. Mar. Sci., 57, 707719. doi:10.1006/jmsc.2000.0734.

Hollowed, A. B., Ianelli, J. N., and Livingston, P. A., 2000b. Including predation mortality in stock assessments: a case study for Gulf of Alaska walleye Pollock. ICES J. Mar. Sci., 57, 279293.

Hollowed, A. B., Curchitser, E. N., Stock, C. A., Zhang, C. 2013. Trade-offs associated with different modeling approaches for assessment of fish and shellfish responses to climate change. Climatic Change 119, 111129 DOI 10.1007/Table 6584-012-0641-z

Holsman, K. K., Ianelli, J., Aydin, K., Punt, A. E., Moffitt , E. A. (2016). Comparative biological reference points estimated from temperature-specific multispecies and single species stock assessment models. Deep Sea Res. II. doi:10.1016/j.dsr2.2015.08.001.

Holsman, K. K. and Aydin, K. 2015. Comparative methods for evaluating climate change impacts on the foraging ecology of Alaskan groundfish. Mar. Ecol. Prog. Ser. DOI 10.3354/mep102

Holsman, KK, EL Hazen, A Haynie, S Gourguet, A Hollowed, S Bograd, JF Samhouri, K Aydin. 2019. Toward climate-resiliency in fisheries management. ICES Journal of Marine Science. 10.1093/icesjms/fsz031

Holsman, K.K., A Haynie, A Hollowed et al. 2020a. Climate-informed multispecies assessment model methods for determining biological references points and Acceptable Biological Catch., 24 September 2020, PROTOCOL (Version 1) available at Protocol Exchange [+https://doi.org/10.21203/rs.3.pex-1084/v1+].

Holsman, K.K., A. Haynie, A. Hollowed, J. Reum, K. Aydin, A. Hermann, W. Cheng, A. Faig, J. Ianelli, K. Kearney, A. Punt. 2020b. Ecosystem-based fisheries management forestalls climate-driven collapse. Nature Communications. DOI:10.1038/s41467-020-18300-3.

Honkalehto, T., Ressler, P.H., Towler, R.H., Wilson, C.D., 2011.Using acoustic data from fishing vessels to estimate walleye pollock (Theragra chalcogramma) abundance in the eastern Bering Sea. 2011. Can. J. Fish. Aquat. Sci. 68, 12311242

Howell, D., Bogstad, B. 2010. A combined Gadget/FLR model for management strategy evaluations of the Barents Sea fisheries. ICES J. Mar. Sci, 67, 000000.

Hunsicker, M. E., Ciannelli, L., Bailey, K. M., Zador, S., Stige, L. C., 2013. Climate and demography dictate the strength of predator-prey overlap in a subarctic marine ecosystem. PloS one 8(6), e66025. doi:10.1371/journal.pone.0066025.

Hunt G. L. Jr, Coyle K. O., Eisner L., Farley E. V., Heintz R., Mueter, F., Napp, J. M., Overland, J. E., Ressler, P. H., Salo, S., Stabeno, P. J., 2011. Climate impacts on eastern Bering Sea foodwebs: A synthesis of new data and an assessment of the Oscillating Control Hypothesis. ICES J. Mar. Sci. 68(6), 12301243.

Ianelli, J. N., Honkalehto T., Barbeaux S., Kotwicki S., 2014. Chapter 1: Assessment of the walleye pollock stock in the Eastern Bering Sea. In Stock Assessment and Fishery Evaluation Report for the Groundfish Resources of the Bering Sea/Aleutian Islands Regions, Alaska Fisheries Science Center, National Marine Fisheries Service, Anchorage, AK, p 55156.

Ianelli, J. N., Barbeaux, S., Honkalehto, T., Kotwicki, S., Aydin, K., and Williamson, N. 2012. Assessment of Alaska Pollock Stock in the eastern Bering Sea. In Stock Assessment and Fishery Evaluation Report for the Groundfish Resources of the Bering Sea/Aleutian Islands Regions, pp. 31124.

Ianelli, J. N., et al. 2019. Assessment of Alaska Pollock Stock in the eastern Bering Sea. In Stock Assessment and Fishery Evaluation Report for the Groundfish Resources of the Bering Sea/Aleutian Islands Regions.

Ianelli, J. N., Holsman, K. K. Punt, A. E., Aydin, K. 2016. Multi-model inference for incorporating trophic and climate uncertainty into stock assessments. Deep Sea Res. II

Jurado-Molina, J., Livingston, P. A., Ianelli, J. N., 2005. Incorporating predation interactions in a statistical catch-at-age model for a predator-prey system in the eastern Bering Sea. Can. J. Fish. Aquat. Sci. 62, 1865-1873.

Kaplan, I. C. , P. J. Horne, P. S. Levin., 2012. Screening California Current fishery manamgent scenarios using the Atlantis end-to-end ecosystem model. Prog. Oceanogr. 102, 5-18.

Kaplan, I.C., Brown, C.J., Fulton, E.A., Gray, I.A., Field, J.C., Smith, A.D.M., 2013. Impacts of depleting forage species in the California Current. Environ. Cons. 40, 380393.

Karp, M ,JO Peterson, PD Lynch, RB Griffis, C Adams, B Arnold, L Barnett, Y deReynier, J DiCosimo, K Fenske, S Gaichas, A Hollowed, K Holsman, + 13. 2019. Accounting for Shifting Distributions and Changing Productivity in the Development of Scientific Advice for Fishery Management. ICES Journal of Marine Science fsz048, https://doi.org/10.1093/icesjms/fsz048

Kearney, K, A. Hermann, W. Cheng, I. Ortiz, and K. Aydin. A coupled pelagic benthic-sympagic biogeochemical model for the Bering Sea: documentation and validation of the BESTNPZ model (v2019.08.23) within a high resolution regional ocean model. Geoscientific Model Development, 13 (2):597–650, 2020. DOI: 10.5194/gmd13-597-2020.

Kinzey, D. Punt, A. E., 2009. Multispecies and single-species age-structured models of fish population dynamics: Comparing parameter estimates. Nat. Res. Mod. 22, 67-104.

Kitchell, J. F., Stewart, D. J. and Weininger, D., 1977. Applications of a bioenergetics model to yellow perch (Perca flavenscens) and walleye (Stizostedion vitreum vitreum). J. Fish. Res. Board Can. 34, 1922-1935.

Levin, P. S., Kelble, C. R., Shuford, R., Ainsworth, C., deReynier, Y., Dunsmore, R., Fogarty, M. J., Holsman, K., Howell, E., Monaco, M., Oakes, S., Werner, F., 2013. Guidance for implementation of integrated ecosystem assessments: a US perspective. ICES J. Mar. Sci, doi:10.1093/icesjms/fst112.

Link J. S., 2010. Ecosystem-based fisheries management: confronting tradeoffs, Cambridge University Press, Cambridge.

Link, J. S., Browman, H. I., 2014. Integrating what? Levels of marine ecosystem-based assessment and management. ICES J. Mar. Sci, 71, 11701173

Livingston, P. A., Aydin, K., Bolt, J. L., Hollowed , A. B., Napp, J. M., 2011. Alaskan marine fisheries management: advances and linkages to ecosystem research. In A Belgrano and W Fowler (eds.), Ecosystem-Based Management for Marine Fisheries: An Evolving Perspective. Cambridge University Press, pp 113-152.

Livingston, P., 1993. Importance of predation by groundfish, marine mammals and birds on walleye pollock Theragra chalcogramma and Pacific herring Clupea pallasi in the eastern Bering Sea. Mar. Ecol. Prog. Ser. 102(3), 205215.

Moffitt, E., Punt, A. E., Holsman, K. K., Aydin, K. Y., Ianelli, J. N., Ortiz, I., 2016. Moving towards Ecosystem Based Fisheries Management: options for parameterizing multispecies harvest control rules. Deep Sea Res. II.

Morita, K., Fukuwaka, M. A., Tanimata, N. and Yamamura, O., 2010. Size-dependent thermal preferences in a pelagic fish. Oikos 119, 1265-1272.

Murawski, S., Matlock G., 2006. Ecosystem science capabilities required to support NOAAs mission in the year 2020. NOAA Technical Memorandum, NMFS-F/SPO-74, Silver Spring, MD.

Mueter, F. J. Megrey, B. A., 2006. Using multispecies surplus production models to estimate ecosystemlevel maximum sustainable yields. Fish. Res. 81, 189201.

Mueter, F. J., Boldt, J. L., Megrey, B. A., Peterman, R. M., 2007. Recruitment and survival of Northeast Pacific Ocean fish stocks: temporal trends, covariation, and regime shifts. Can. J. Fish. Aquat. Sci. 64(6), 911-927.

Mueter, F. J., Bond, N. A., Ianelli, J. N., & Hollowed, A. B. (2011). Expected declines in recruitment of walleye pollock (Theragra chalcogramma) in the eastern Bering Sea under future climate change.

Nishiyama, T., Hirano, K., and Haryu, T., 1986. The early life history and feeding habits of larval walleye pollock Theragra chalcogramma (Pallas) in the southeast Bering Sea. Int. North Pac. Fish. Comm. Bull. 45, 177227.

North Pacific Fishery Management Council (NPFMC). 2013. Fishery Management plan for groundfish of the Bering Sea and Aleutian Islands management area. North Pacific Fishery Management Council, Anchorage, AK.

Ortiz, I, K. Aydin, A. J. Hermann, G. Gibson. 2016. Climate to fisheries: Exploring processes in the eastern Bering Sea based on a 40 year hindcast. Deep Sea Res. II.

Pauly, D., 1981. The relationship between gill surface area and growth performance in fish: a generalization of von Bertalanffys theory of growth. Meeresforschung 28, 251-282.

Plaganyi, ??. E., Punt, A.E., Hillary, R., Morello, E.B., Th??baud, O., Hutton, T., Pillans, R.D., Thorson, J.T., Fulton, E. A., Smith, A. D. M., Smith, F., Bayliss, P., Haywood, M., Lyne, V., Rothlisberg, P.C., 2014. Multispecies fisheries management and conservation: tactical applications using models of intermediate complexity. Fish Fish. 15, 1-22.

Pikitch E. K., Santora C., Babcock E. A., Bakun A., Bonfi, R., Conover, D. O., Dayton, P., Doukakis, P., Fluharty, D., Heneman, B., Houde, E. D., Link, J., Livingston, P. A., Mangel, M., McAllister, M. K., Pope, J., Sainsbury, K. J., 2004. Ecosystem-based fishery management. Science 305, 346347

Punt, A.E., Smith, A.D.M., Smith, D.C., Tuck, G., Klaer, N., 2014. Selecting relative abundance proxies for BMSY and BMEY. ICES J. Mar. Sci. 71, 469-483.

Quinn, T. J., II, Deriso, R. B., 1999. Quantitative Fish Dynamics. Oxford University Press, New York.

Ricker, W. E. (1954) Stock and Recruitment Journal of the Fisheries Research Board of Canada, 11(5): 559623. doi:10.1139/f54-039

Siddon E. C., Kristiansen T., Mueter F. J., Holsman K. K., Heintz R. A., Farley, E. V., 2013. Spatial Match-Mismatch between Juvenile Fish and Prey Provides a Mechanism for Recruitment Variability across Contrasting Climate Conditions in the Eastern Bering Sea. PLoS ONE 8(12), e84526. doi:10.1371/journal.pone.0084526

Smith, M. D., Fulton, E. A., and Day, R.W. 2015. An investigation into fisheries interaction effects using Atlantis. ICES J. Mar. Sci, 72(1), 275283. doi:10.1093/icesjms/fsu114

Spencer, PD, KK Holsman, S Zador, NA Bond, FJ Mueter, AB Hollowed1, and JN Ianelli. (2016). Modelling spatially dependent predation mortality of eastern Bering Sea walleye pollock, and its implications for stock dynamics under future climate scenarios. ICES Journal of Marine Science; doi:10.1093/icesjms/fsw040

Spies, I. Wilderbuer, T. K., Nichol, D. G. and Aydin, K., 2012. Chapter 6. Arrowtooth Flounder. In Stock Assessment and Fishery Evaluation Report for the Groundfish Resources of the Bering Sea/Aleutian Islands Regions, pp. 31124.

Spies, I. et al. Genetic evidence of a northward range expansion in the eastern Bering Sea stock of Pacific cod. Evol. Appl. 13, 362–375 (2020).

Stabeno, P.J., Farley, E.V., Jr., Kachel, N.B., Moor, S., Mordy, C.W., Napp, J.M., Overland, J.E., Pinchuk, A.I., Sigler, M.F., 2012. A comparison of the physics of the northern and southern shelves of the eastern Bering Sea and some implications for the ecosystem. Deep Sea Res. II 65-70, 14-30.

Stevenson, D. E. & Lauth, R. R. Bottom trawl surveys in the northern Bering Sea indicate recent shifts in the distribution of marine species. Polar Biol. 42, 407–421 (2019).

Taylor, L. , Begley, J., Kupca1, V. Stefansson, G., 2007. A simple implementation of the statistical modelling framework Gadget for cod in Icelandic waters. Afr. J. Mar. Sci., 29(2), 223245

Temming, A., 1994. Food conversion efficiency and the von Bertalanffy growth function. Part II and conclusion: extension of the new model to the generalized von Bertalanffy growth function. NAGA The ICLARM Quarterly, 17(4), 41-45.

Tsehaye, I., Jones, M. I., Bence, J. R., Brenden, T. O., Madenjian, C. P., Warner, D. M., 2014. A multispecies statistical age-structured model to assess predator-prey balance: application to an intensively managed Lake Michigan pelagic fish community. Can. J. Fish. Aquat. Sci. 71, 627-644.

Thompson, G. G., Lauth, R. R., 2012. Chapter 2: Assessment of the Pacific Cod Stock in the Eastern Bering Sea and Aleutian Islands Area. In Stock Assessment and Fishery Evaluation Report for the Groundfish Resources of the Bering Sea/Aleutian Islands Regions, pp. 31124.

Tyrrell M. C., Link J. S., Moustahfid H., 2011. The importance of including predation in some fish population models: implications for biological reference points. Fish. Res. 108, 1-8.

Van Kirk, K. F., Quinn II, T. J., Collie, J. S., 2010. A multispecies age-structured assessment model for the Gulf of Alaska. Can. J. Fish. Aquat. Sci. 67, 1135-1148.

von Bertalanffy, L., 1938. A quantitative theory of organic growth. Hum. Biol. 10: 181-213.

Worm B., Hilborn R., Baum J. K., Branch T. A. Collie, J. S., Costello, C., Fogarty, M. J., Fulton, E. A., Hutchings, J. A., Jennings, S., Jensen, O. P., Lotze, H. K., Mace, P. M., McClanahan, T. R., Minto, C.,

Palumbi, S. R., Parma, A. M., Ricard, D. , Rosenberg, A. A., Watson, R., Zeller, D., 2009. Rebuilding global fisheries. Science 325, 578585

Zador S., Aydin K., Cope J., 2011. Fine-scale analysis of arrowtooth flounder Atherestes stomias catch rates reveals spatial trends in abundance. Mar. Ecol. Prog. Ser. 438, 229-239

9 Figures & Tables

Table 6. Proportion mature (ρ_{ij}) and residual natural mortality ($\mathrm{M1}_{ij}$) for each species i and age j in the single-species (SSM) or multi-species model (MSM) for wallleye pollock (plk), Pacific cod (pcod), and Arrowtooth flounder (atf).

Age	1	2	3	4	5	6	7	8	9	10	11	12	13	14	15	16	17	18	19	20	21
ρ_{ij}																					
plk	0.00	0.01	0.29	0.64	0.84	0.90	0.95	0.96	0.97	1.00	1.00	1.00									
pcod	0.00	0.02	0.06	0.14	0.30	0.53	0.75	0.89	0.95	0.98	0.99	1.00									
atf	0.00	0.00	0.01	0.02	0.06	0.16	0.34	0.59	0.80	0.92	0.97	0.99	1.00	1.00	1.00	1.00	1.00	1.00	1.00	1.00	1.00
SSM $\mathrm{M1}_{ij}$																					
plk	0.90	0.45	0.30	0.30	0.30	0.30	0.30	0.30	0.30	0.30	0.30	0.30									
pcod	0.34	0.34	0.34	0.34	0.34	0.34	0.34	0.34	0.34	0.34	0.34	0.34									
atf	0.27	0.26	0.26	0.25	0.25	0.24	0.24	0.23	0.23	0.23	0.22	0.22	0.22	0.22	0.21	0.21	0.21	0.21	0.21	0.21	0.21
MSM $\mathrm{M1}_{ij}$																					
plk	0.01	0.30	0.30	0.30	0.30	0.30	0.30	0.30	0.30	0.30	0.30	0.30									
pcod	0.34	0.34	0.34	0.34	0.34	0.34	0.34	0.34	0.34	0.34	0.34	0.34									
atf	0.27	0.26	0.26	0.25	0.25	0.24	0.24	0.23	0.23	0.23	0.22	0.22	0.22	0.22	0.21	0.21	0.21	0.21	0.21	0.21	0.21

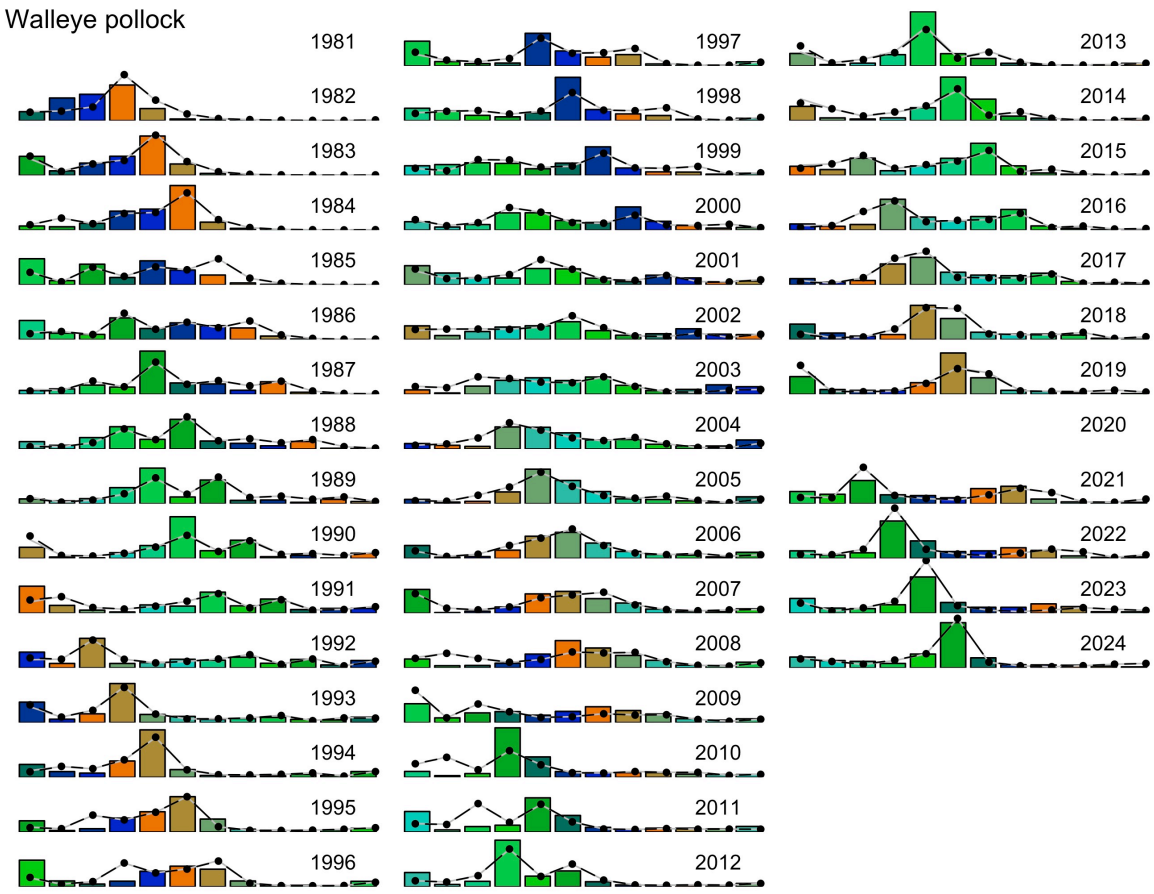

Figure 26: Survey age compostitions for walleye pollock. Bars represent observed values, black and gray points represent single- and multispecies fits to the data, respectively.

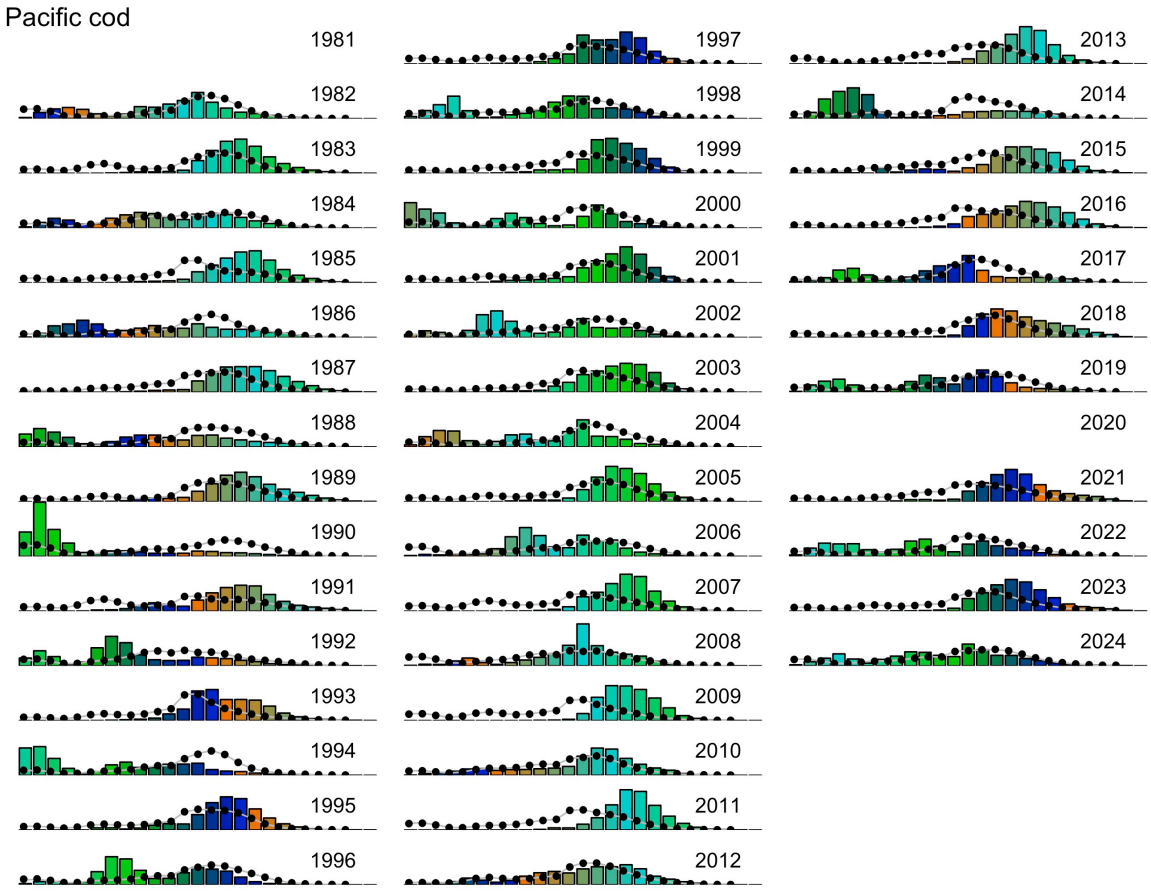

Figure 27: Survey length compostitions for Pacific cod Bars represent observed values, black and gray points represent single- and multispecies fits to the data, respectively.

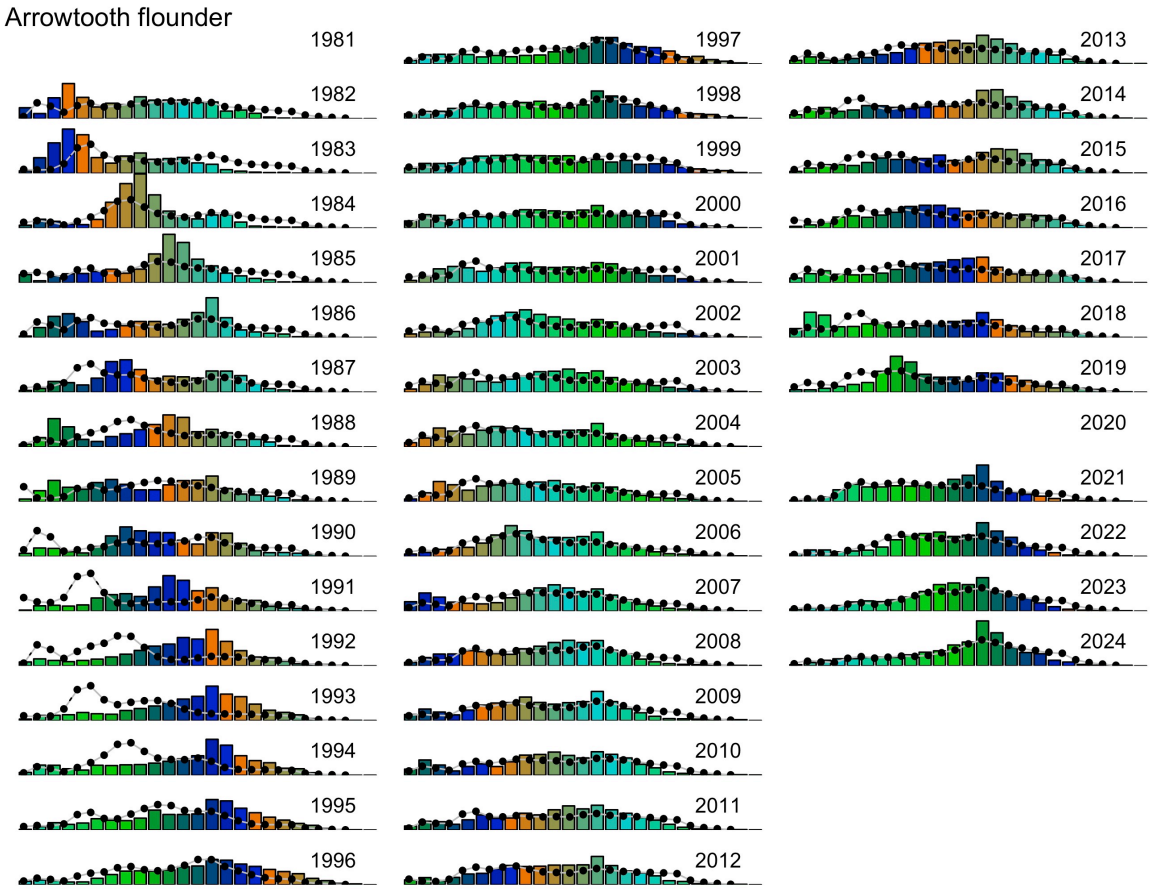

Figure 28: Survey length compostitions for arrowtooth flounder Bars represent observed values, black and gray points represent single- and multispecies fits to the data, respectively.

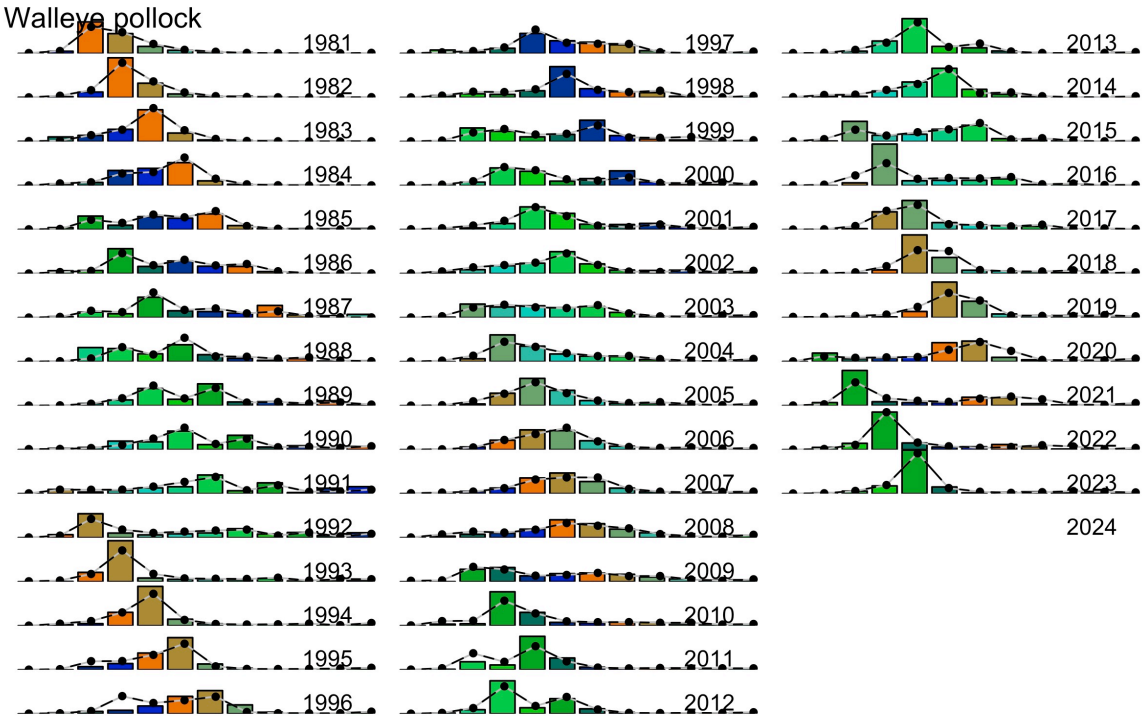

Figure 29: Fishery age compostitions for walleye pollock. Bars represent observed values, black and gray points represent single- and multispecies fits to the data, respectively.

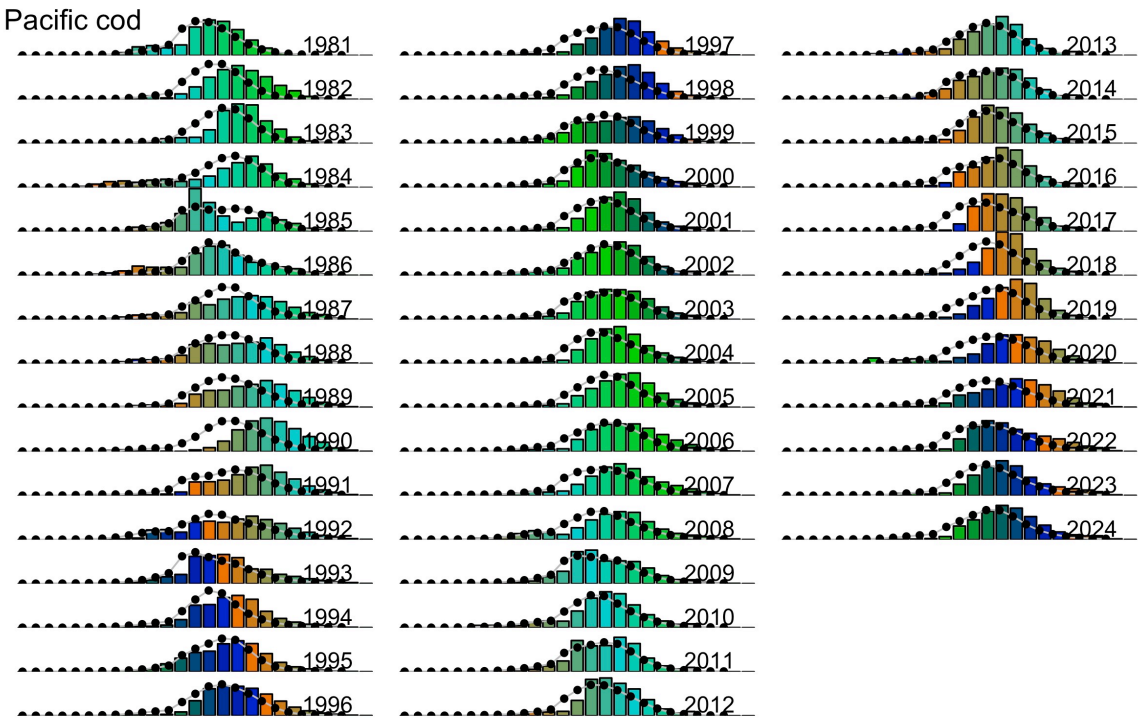

Figure 30: Fishery age compostitions for Pacific cod. Bars represent observed values, black and gray points represent single- and multispecies fits to the data, respectively.

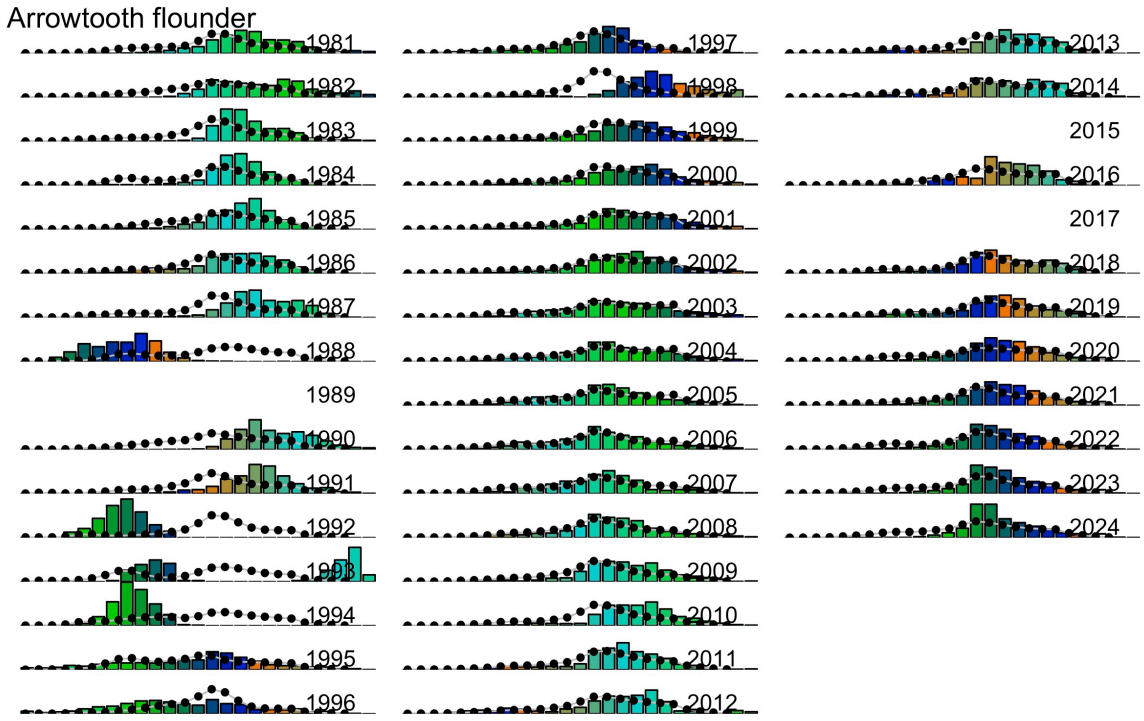

Figure 31: Fishery age compostitions for arrowtooth flounder. Bars represent observed values, black and gray points represent single- and multispecies fits to the data, respectively.

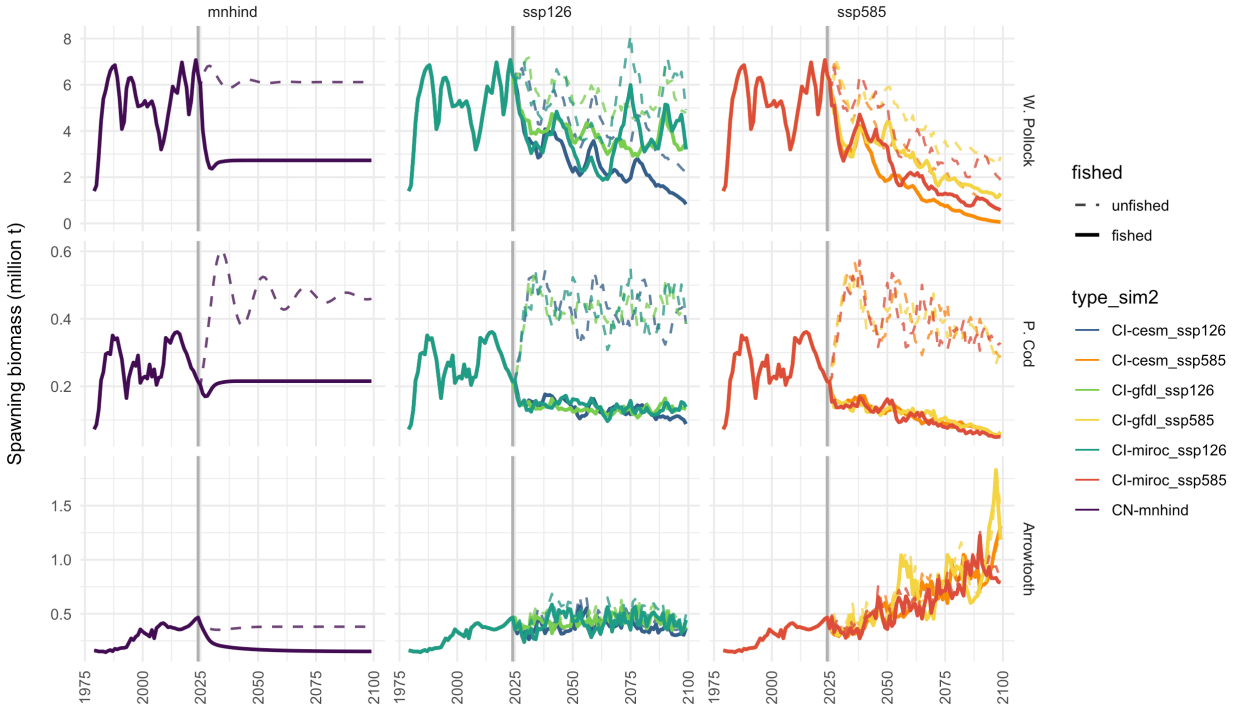

Figure 32: Single-species CEATTLE model projections of unfished (B0, dashed lines) and fished spawning stock biomass at the harvest rate corresponding to the ABC proxy (B40, solid lines) for the climate naive scenario (mnhind), high carbon mitigation (ssp126) and low carbon mitigation (ssp585) scenarios. B0 from the climate naive model (left panel) was used to determine the target biomass B40 each species (rows). The lines in the two carbon mitigation scenarios represent different (earth system model) realizations which differentially impact recruitment and weight at age in the model. Harvest is set at Ftarget for each species.Projections assume no adaptation by the species, fishery, or fishery management. See Holsman et al. 2020 for more information and climate informed projections.

Figure 33: Multi-species CEATTLE model projections of unfished (B0, dashed lines) and fished spawning stock biomass at the harvest rate corresponding to the ABC proxy (B40, solid lines) for the climate naive scenario (mnhind), high carbon mitigation (ssp126) and low carbon mitigation (ssp585) scenarios. B0 from the climate naive model (left panel) was used to determine the target biomass B40 each species (rows). The lines in the two carbon mitigation scenarios represent different (earth system model) realizations which differentially impact recruitment and weight at age in the model. Harvest is set at Ftarget for each species.Projections assume no adaptation by the species, fishery, or fishery management. See Holsman et al. 2020 for more information and climate informed projections.

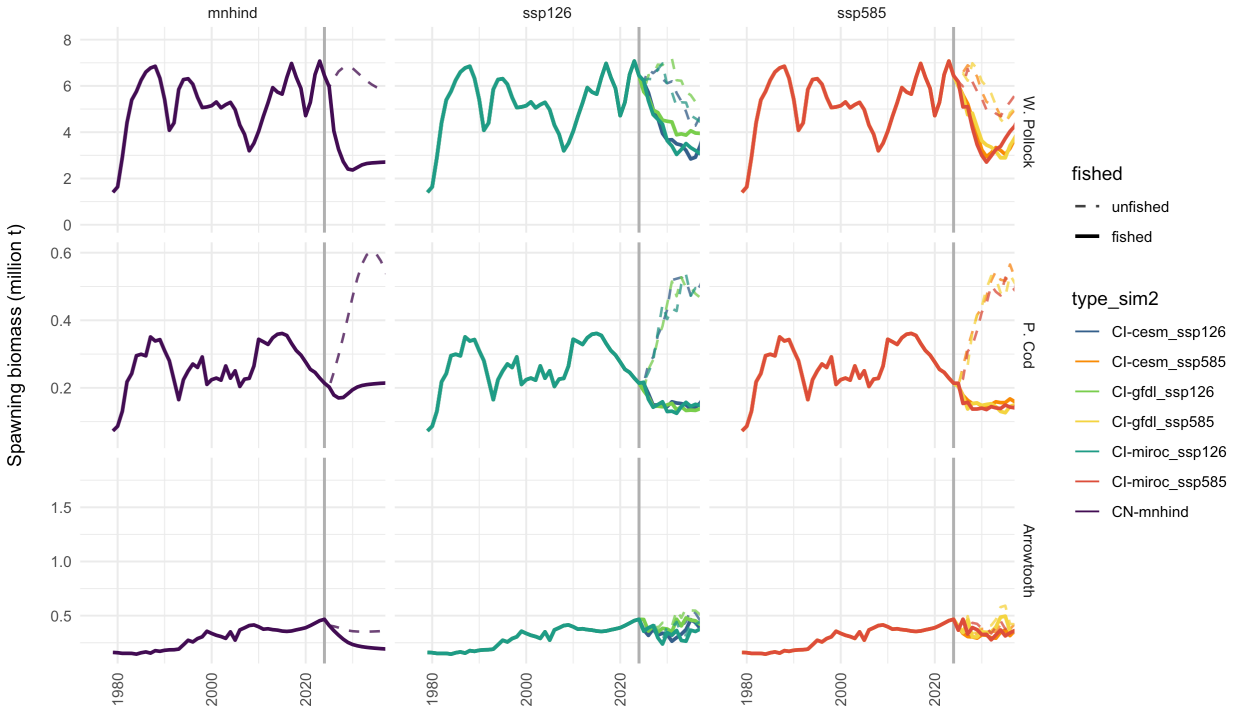

Figure 34: As in previous figures but with closer detail at this year. Spawning stock biomass for each species at the start of each model year (single-species). Vertical line represents end of this year and the start of next year

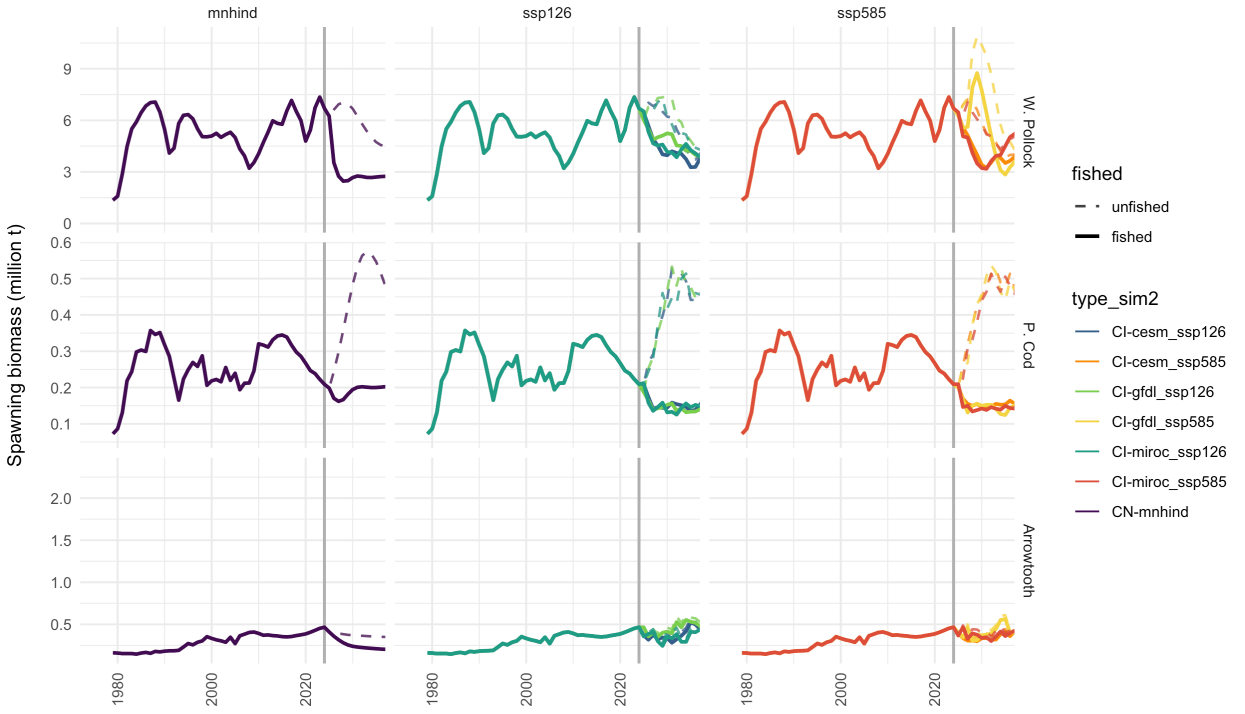

Figure 35: As in previous figures but with closer detail at this year. Spawning stock biomass for each species at the start of each model year (multi-species). Vertical line represents end of this year and the start of next year

	Walleye pollock	Pacific cod	Arrowtooth flounder
α	0.006	0.004	0.005
β	3.04	3.22	3.175
C_A	0.119	0.041	0.125
C_B	−0.46	−0.122	−0.199
C_Q	2.6	2.41	2.497
T_{C_o}	10	13.7	20.512
T_{C_M}	15	21	26
RFR_{juv}			
EBS	0.41	0.68	0.83
AI	0.24	0.48	0.52
GOA	0.49	0.41	0.79
RFR_{adult}			
EBS	0.79	1.57	1.29
AI	0.72	0.68	1.22
GOA	0.56	0.47	1.07
H			
EBS	11.798	8.691	4.651
AI	28.816	8.691	3.443
GOA	9.008	17.628	5.397
k			
EBS	0.375	0.511	1.235
AI	0.422	0.511	0.531
GOA	2.036	0.133	0.355
a_0			
EBS	0.357	−0.259	−1.495
AI	0.486	−0.259	−2
GOA	−0.445	0.115	−0.618
d			
EBS	0.548	0.715	0.835
AI	0.428	0.715	0.776
GOA	0.796	0.544	0.673
H_{spec}			
EBS	8.214	10.176	6.392
AI	11.869	12.468	4.583
GOA	11.669	10.613	5.502
k_{spec}			
EBS	0.672	0.33	0.405
AI	1.05	0.42	0.269
GOA	1.001	0.414	0.341
$a_{0\text{spec}}$			
EBS	0.025	−0.06	−0.049
AI	−0.018	−0.029	−0.84
GOA	0.078	−0.275	−0.577

Figure 36: Temperature-dependent Von Bertalanffy parameter (parm) estimates, standard deviation in parameter estimates (stdev), and confidence intervals (CI) from Holsman and Aydin, 2015.